Review of the state of art of Li-based inhibitors and coating technology for the corrosion protection of aluminium alloys

Li, Ziyu; Visser, Peter; Hughes, Anthony E.; Homborg, Axel; Gonzalez-Garcia, Yaiza; Mol, Arjan

DOI
10.1016/j.surfcoat.2024.130441

Publication date
2024

Document Version
Final published version

Published in
Surface and Coatings Technology

Surface & Coatings Technology 478 (2024) 130441

Contents lists available at ScienceDirect

Surface & Coatings Technology

journal homepage: www.elsevier.com/locate/surfcoat

Review of the state of art of Li-based inhibitors and coating technology for the corrosion protection of aluminium alloys

Ziyu Li [a], Peter Visser [b], Anthony E. Hughes [c], Axel Homborg [a,d], Yaiza Gonzalez-Garcia [a], Arjan Mol [a,*]

[a] Delft University of Technology, Department of Materials Science and Engineering, Mekelweg 2, 2628CD Delft, the Netherlands
[b] AkzoNobel, Rijksstraatweg 31, 2171 AJ Sassenheim, the Netherlands
[c] CSIRO Mineral Resources, Clayton, Vic 3168, Australia
[d] Netherlands Defence Academy, Het Nieuwe Diep 8, 1781 AC Den Helder, the Netherlands

ARTICLE INFO

Keywords:
lithium inhibitor
Corrosion protection
Aluminium alloy
Coating technology

ABSTRACT

The quest for novel alternatives to hexavalent-chromium-based corrosion inhibitors is of utmost significance and urgency. Strict international health and safety regulations, due to growing concerns regarding the impact of hexavalent chromium on human health and the environment, have pushed the commercial introduction of many alternative inhibitor types, but the implementation of alternative active protective primers for structural parts in the aerospace industry is still pending. This endeavour has proven to be remarkably challenging, as the potential replacement coating types must meet numerous functional requirements encompassing cost-effectiveness and exceptional corrosion protection for intrinsically corrosion susceptible aerospace aluminium alloys. In recent years, considerable attention has been drawn to lithium salts as environmentally friendly corrosion inhibitors forming the basis for a novel active protective coating technology. The involvement of lithium ions has been shown to play a pivotal role in the conversion process of aluminium alloy surfaces by stabilizing the reaction products, thereby facilitating the gradual development of a protective layer with a multi-layered configuration, which exhibits considerable variability in morphology, depending on local chemical and electrochemical conditions. The versatility of the lithium-based corrosion protection extends to their application as corrosion inhibiting pigments in organic coatings or as a pre-treatment, directly forming conversion layers, thereby enhancing their practical implementation. However, previous chromate replacement reviews only introduced the promising outcomes provided by the lithium technology, omitting key details of its development and formation mechanism. This paper critically reviews and summarizes the studies conducted to date on lithium-based inhibitor technologies for the corrosion protection of aluminium alloys as well as topics to be investigated in the future.

1. Introduction

Aerospace aluminium alloys have found extensive use in the aerospace industry and other transport sectors due to their notably high strength-to-weight ratio, favourable elastic moduli, malleability, formability, and cost-effectiveness [1–4]. Alloying elements which form various hardening precipitates significantly enhance the mechanical properties of aluminium alloys [5]. However, the addition of multiple elements also contributes to a complex and highly heterogeneous microstructure which makes aluminium alloys susceptible to localized corrosion [4,6–8]. Therefore, the corrosion protective demands in practical applications for reliable and effective pre-treatments and coatings applied to aluminium alloys are enormous [9]. For decades, the application of hexavalent-chromium-based inhibitors by spraying or immersing metallic parts into chromate-based aqueous solutions and by leaching from chromate-containing organic coatings for the protection of aluminium alloys have been a reliable corrosion protection strategy with an extensive track record [10–14]. Hexavalent chromium compounds have long been used as effective inhibitors due to their ability to form a dense, active and self-healing corrosion protective layer on the surface of various aluminium alloys, providing excellent corrosion protection [15]. However, the toxicity and environmental concerns

* Corresponding author.
E-mail address: J.M.C.Mol@tudelft.nl (A. Mol).

https://doi.org/10.1016/j.surfcoat.2024.130441
Received 30 December 2023; Accepted 15 January 2024
Available online 23 January 2024

associated with hexavalent chromium inhibitors have led to a growing and urgent demand for alternative, environmentally friendly inhibitors [13,16].

In response to this demand, significant efforts have been implemented for the exploration of chromate-free protective schemes for industrial applications. These processes can be mainly divided into two groups: chromate-free pre-treatments and chromate-free organic coatings [17–24]. Ideally, these alternative processes should exhibit similar performances to chromates, i.e., providing effective corrosion protection to the substrate under various harsh service environments and manifesting self-healing properties when defects are generated on the protected surfaces. For surface treatments, various technologies including molybdate [25], vanadate [26], permanganate [27], phosphates [28], silanes [29], sol-gels [30], and rare earth-based compounds [31,32] etc. for chemical conversion coatings, have been proposed. As for organic coating systems, most of the recommended inhibitors are inorganic based, such as vanadate [33] and praseodymium [34] as leaching inhibitors, and Mg-rich or Al-rich primers [35,36] as galvanic inhibition strategies. Lithium (Li) salts possess the advantages of being promising candidates, both as chemicals for conversion treatments [20,37,38] and as compounds that are leachable from organic coatings [39–43].

The introduction of Li in the scope of pretreatments dates back to the 1980s when Gui and Devine [38] generated a Li-based conversion layer on AA6061-T6 by applying anodic polarization in a deaerated Li_2CO_3 solution. The resulting passivation effect was not observed when the panels were tested in Li-free carbonate solutions. Similarly, local passivation of the crack wall observed from Al-Li alloy 2090 was enabled under an alkaline and CO_2-bearing environment [44], but this dilute Li containing environment could not generate a uniform passivation layer over the entire alloy surface. Rangel and Travassos [45,46] then provided evidence for the irreversible formation of a Li-based conversion layer, applied in a conversion bath of 0.5 M Li_2CO_3, using cyclic voltammetry on pure aluminium coupons. In addition, it was also noticed that the presence of oxygen is a key factor for the growth of the Li-based conversion layer under open circuit potential (OCP) conditions. Besides the commonly employed Li_2CO_3, LiOH or Li_2SO_4 were noted to enable passivation of aluminium alloys as well [45,46]. A detailed compositional analysis, conversion process optimization and surface modifications were reported by the pioneering work from Buchheit et al. [20,21,37,47–55] for a variety of commercial aluminium alloys. In the beginning, using a higher concentration (0.1 M) of Li_2CO_3 combined with LiOH for pH adjustment, an immersion duration of 15 min under OCP was applied to produce an effective protective film, which made it more suitable for industrial applications. However, this process duration is still longer than traditional chromate-based conversion treatments, which is usually $\leq$ 180 s at ambient conditions [56]. X-ray diffraction analysis revealed that the composition of the film was mainly polycrystalline $Li_2\left[Al_2(OH)_6\right]_2CO_3{\cdot}nH_2O$, which is a common Li/Al layered double hydroxide (LDH) layer [37,57]. Later, further studies indicated that elevating the conversion bath temperature, the addition of oxidizing agents to the conversion bath and post heat treatment of the freshly-formed conversion layer in air or distilled water, produced a film with a higher corrosion resistance by effectively reducing the porosity of the conversion layer [54]. Furthermore, the addition of transition- or rare earth compounds into the freshly-formed conversion layer provides the LDH layer with enhanced corrosion protection and self-healing abilities [58–60]. For instance, it was shown that a Li/Al LDH-based conversion layer sealed by immersion in Ce-containing solutions, exhibits self-healing behaviour due to the presence of Ce ions [61]. Earlier studies were usually performed at a relatively high concentration and high pH of Li_2CO_3 (e.g., 0.05 M or 0.1 M) [38].

The protective layer formation process by leaching from coatings shows notable differences compared to that for the "static" conversion process within the electrochemical cell. Immersion of aluminium alloys in a lower concentration of Li_2CO_3 (0.01 M) was investigated only recently, since this specified concentration was believed to be comparable to the local concentration of Li_2CO_3 within an exposed artificial scratch in an organic coating, loaded with Li_2CO_3 [62–65]. In other words, a simplified environment was created to mimic the local environment involving a complex organic coating system. An artificial scratch deep into the alloy surface was created to evaluate the active corrosion protection process [39,40]. Visser et al. [39,66] have incorporated Li salts, such as Li_2CO_3 and Li-oxalate in polyurethane and epoxy coatings and studied the leaching of the Li ions and the active corrosion protective properties in a scribe after exposure to continuous salt spray testing (ASTM B117) and demonstrated the formation of a protective Li-containing layer. Marcoen et al. [67] monitored the leaching of Li salts into a coating defect as a function of salt spray exposure time by time-of-flight secondary ion mass spectrometry (ToF-SIMS). The scribes were completely covered with a Li-containing protective layer within 15 min. Initially, a Li-pseudoboehmite barrier layer formed on the substrate surface and after longer exposure times, Li/Al LDH started to form and eventually covered the surface. Trentin et al. [68] investigated the role of Li salts in PMMA-silica coatings. They found that increasing the Li_2CO_3 loading could enhance the corrosion protection, and the incorporation of Li ions resulted in significant modification of the hybrid structure through the formation of a dense and highly cross-linked hybrid network. Subsequent work studied the ion transport pathways within the organic coating and revealed its complex diffusion mechanism [69,70]. These studies enable researchers to understand how Li-based inhibitors are delivered from the primer matrix when exposed to an electrolyte and hence allow the further development of a complex coating constitution for optimal leaching kinetics. Apart from the corrosion protection of aerospace aluminium alloys, applications of Li salts to Portland cement paste containing an aluminium substrate were reported recently [71]. AA1100 encapsulated in Portland cement pastes is effectively protected with the addition of $LiNO_3$ or Li_2CO_3 through the formation of a protective film.

More recently studies of the Li-based conversion process already have moved into the microscale or nanoscale level to help elucidate the mechanism of the growth stages and influential factors which are important for the realization of a relatively fast formation rate and enhanced corrosion protection [72]. Fig. 1 summarizes (i) the performance and formation mechanism of the Li-based conversion coatings, (ii) the performance and action of inhibitors at Li leaching organic coating defects, and (iii) its in-coating mobility and leaching properties based on previous work, which will be subsequently presented in further detail in the next sections. Finally, this review provides a concise outlook on the overall applications of Li salts for the corrosion protection of aluminium alloys.

2. Li-based chemical conversion coating performance and mechanism

LDH materials represent a class of compounds categorized as anionic clays, exhibiting intricately adjustable brucite-like structures [73]. These compounds exhibit a distinct arrangement wherein mixed metal M^I/M^{II} and M^{III}/M^{IV} hydroxide layers exhibit a positive charge, which is counterbalanced by anions (denoted as A^{y-}) and water molecules within the interlayered region. The major group of LDHs can be formulated as $\left[M^{II}_{1-x}M^{III}_x(OH)_2\right]^{x+}(A^{y-})_{x/y}{\cdot}nH_2O$, where M^{II} and M^{III} are divalent and trivalent metal cations, respectively, and A^{y-} represents the interlayer anions, x is in the range of 0.22–0.33 [74]. The isomorphous replacement of trivalent cations for divalent cations in the hydroxide layer of LDHs leads to excess positive charges in the layer. LDH chemical conversion coatings have attracted attention recently as corrosion protective films for various metal substrates [75–79]. LDHs have gained significant attention in the realm of corrosion protection owing to their characteristics including cost-effectiveness, high surface area, favourable adhesion to substrates, eco-friendly nature, ion-exchange

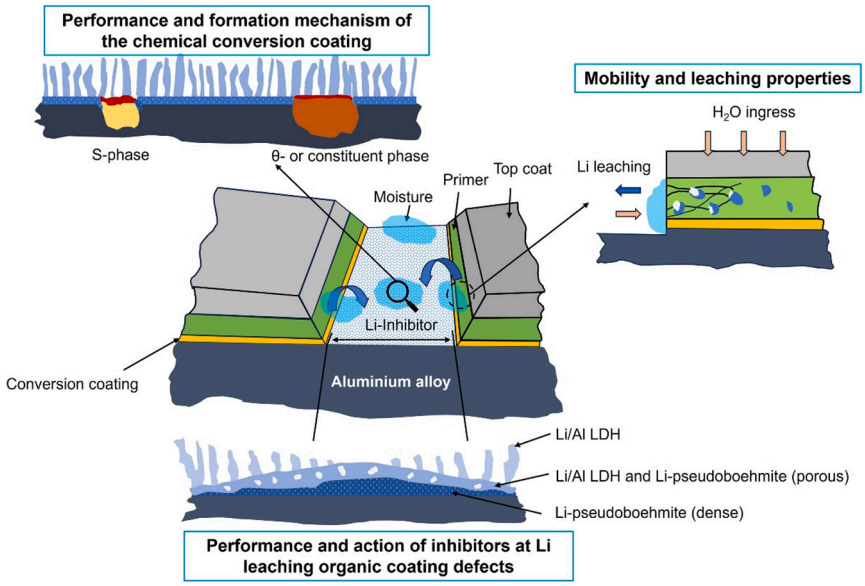

Fig. 1. Li-based inhibitors and coating technology including (i) the performance and formation mechanism of the chemical conversion coating, (ii) the performance and action of inhibitors at Li leaching organic coating defects, and (iii) the mobility and leaching properties of Li salts.

capabilities, self-healing, and the accessibility of a diverse array of anionic and cationic components [80–82]. For instance, a Zn/Al LDH layer was synthesized on AA2024-T3 including the intercalation of the inhibitor diethyldithiocarbamate through an ion-exchange procedure, which provided active corrosion protection to the substrate [82]. Vieira et al. [83] reported that the corrosion protection provided by the Mg/Al LDH conversion coating could be extended by the release of incorporated Ce ions. Except for serving as a physical barrier layer, LDH particles could be doped into sol-gel coating systems to enhance the corrosion protection through absorbing aggressive anion ions or releasing stored inhibitors [84–86].

In addition to M^{II}/M^{III} compositional LDHs, another distinct category of LDHs is represented by Li/Al LDHs, bearing the formula $\left[LiAl_2(OH)_6\right]^+A^{y-}_{1/y}\cdot nH_2O$. Within the framework of the Li/Al LDH structure, the Li cations are positioned in the unoccupied octahedral sites within the aluminium hydroxide layer, where the aluminium ions occupy two-thirds of these octahedral sites, thereby contributing to the positive charges characterizing the hydroxide layer [74]. The process of intercalating Li salts into the structures necessitates the perturbation of the hydrogen bonding networks, along with the reconfiguration of the hydroxide layers. Notably, a previously reported activation energy of 27 kJ mol^{-1} has been associated with the intercalation reaction of gibbsite involving Li species [87]. In addition, the intercalation process is reversible. For instance, the de-intercalation process occurs when the freshly-formed Li/Al LDH is exposed to a Li-free liquid environment leading to crystalline aluminium hydroxide products [88]. A detailed structure of Li/Al LDHs and its de-intercalation through calcination is provided in Fig. 2 [89]. The reversible intercalation capability has been widely used in the extraction and collection of Li ions from salt lake brines [90–92]. It has been reported that the Li/Al LDH layer retains the highest charge density of all LDHs, thus indicating a higher anion exchange capacity as compared to other types of LDHs [93].

LDH conversion coatings grown on metallic substrates can be prepared generally using one step in-situ growth or co-precipitation methods [94]. The process of co-precipitation is based on crystallization of LDH in an alkaline solution containing M^I and/or M^{II} and M^{III} cations precursors. The metal substrate is also a source of metal cations. However, for the case of one step in-situ growth method, all cations must originate from the metal substrate, which makes it limited to certain

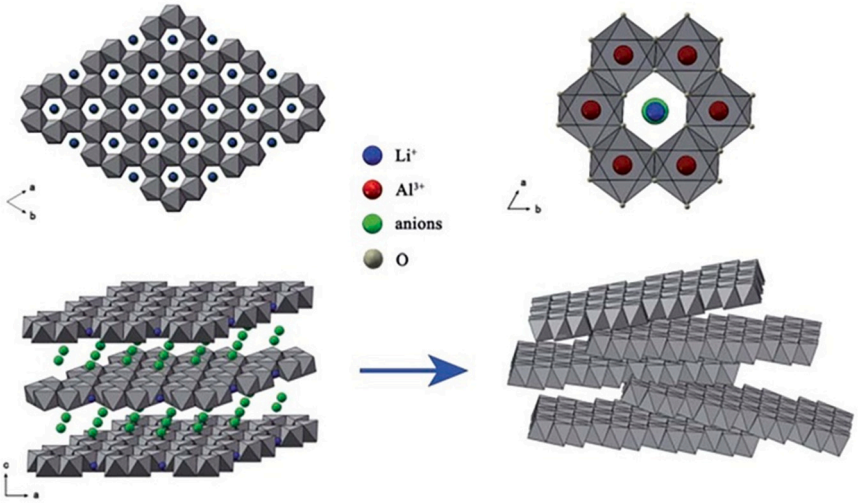

Fig. 2. Crystal structure of Li/Al LDH and its de-intercalation process. Reprinted from [89] with permission from the Royal Society of Chemistry.

alloys. Heating usually is necessary for the effective crystallization of LDH coatings for which temperature elevation, hydrothermal growth, and steam treatment are common heating procedures [94].

One performance criterion for Li-based conversion layers is their stand-alone corrosion protection. Multiple tests performed by Buchheit et al. [47,50,51] like salt spray testing, potentiodynamic polarization, and electrochemical impedance spectroscopy (EIS) were used to evaluate the performance of the Li-based conversion layer in order to determine its eligibility for substituting traditional hexavalent chromium. The structure, properties and performance of the Li-based conversion layers strongly depend on the bath chemistry. For instance, the addition of LiOH for pH adjustment, of aluminate salts for promoting the precipitation, and of oxidants for improving the oxidizing power are necessary to develop high quality conversion layers; the conversion bath solely containing Li_2CO_3 cannot reach the benchmark set by traditional hexavalent-chromium-based inhibitors [54]. It was observed that the conversion layer improved the corrosion resistance by inhibiting both anodic and cathodic reactions due to the uniformly grown film covering both the aluminium matrix and intermetallic particles (IMPs) [48]. The corrosion protection provided by the conversion layer was sufficient to inhibit pitting corrosion on AA1100 and AA6061-T6 during ASTM B-117 salt spray exposure but failed to provide effective protection on AA2024-T3 based on identical conversion bath procedures, due to the higher Cu content of the latter [48]. In general, the corrosion protection provided by the conversion layers grown over AA2024-T3 is more difficult to pass the salt spray test requirements compared to that of AA6061-T6 under the same procedures since AA2024-T3 is intrinsically less corrosion resistant [50]. Thickening the conversion layer by extending the immersion duration, removing the enriched surface Cu during the conversion growth process, or sealing by incorporating other inhibitors are effective corrosion protection methods to withstand salt spray exposure especially for aluminium alloys with high Cu content [52]. Another factor that should be paid attention to is the self-healing property of the conversion layer. Buchheit et al. [54] observed that AA2024-T3 panels treated in the lithium salt bath containing oxidizing agents presented an increased low-frequency impedance modulus value with exposure time. This “healing” effect may be attributed to the low-temperature hydrothermal sealing of the coating. Another possible reason is that LDH layers can serve as chloride ion sorbent due to their anion exchange abilities. By this way, the chloride scavenging effect hinders chloride ions to reach the surface of the substrate [95,96]. Yan et al. [97] observed the self-healing capacity of a Zn/Al LDH grown on pure aluminium substrates. This self-healing was due to the local dissolution of the original Zn/Al LDH close to the scratch upon exposure to the corrosive electrolyte, which provided suitable conditions for the recrystallization of the Zn/Al LDH at the defect. This mechanism was also postulated to explain the self-healing ability of certain Li/Al LDHs [98,99]. In summary, Li-based conversion layers may be able to provide stand-alone corrosion protection comparable to that provided by traditional hexavalent-chromium-based chemistries, but at the cost of longer immersion time, relatively high energy consumption for application at elevated temperatures and complex and strict application procedures, which may have hampered its introduction in industrial applications. The demonstrated self-repair capability of LDH conversion coatings [97–99] suggests that effective corrosion protection can be achieved even without external inhibitor intercalation; however, a more in-depth exploration of its corrosion protection efficiency is still needed.

The formation process of the Li-based conversion layer includes a rapid dissolution caused by the highly aggressive (pH 13) conversion bath followed by a protective conversion layer growth covering the entire alloy surface. Rangel and Travassos [45,46] predicted a dual structure of the conversion layers through the interpretation of EIS spectra which was confirmed by Buchheit et al., however, the thickness of the dense layer is very thin under high alkaline conditions [37,52]. Experimental studies have revealed that the aluminium surface undergoes mainly two dissolution and one precipitation stage when exposed to water or alkaline environments: (i) the dissolution of a naturally formed oxide layer and the appearance of an amorphous hydroxide layer, (ii) the dissolution of the amorphous layer to aluminate species, and (iii) the precipitation of these species as hydroxide products [50,100]. As a result, a dual layer with a poorly crystalline boehmite or pseudoboehmite inner barrier layer and a crystal boehmite or bayerite (longer ageing times) outer non-barrier layer. Pseudoboehmite here is more prevalent since it forms rapidly but not readily crystallizes [50]. A highly alkaline solution does not change this procedure but accelerates the dissolution and postpones the precipitation due to a higher solubility of aluminate ions. The presence of Li ions in alkaline solutions also does not change this reaction sequence but will alter the precipitation products, resulting in a more corrosion protective film. Previous studies showed that the outer Li/Al LDH layer here was merely a minor corrosion barrier, the inner layer was the dominant contributor for corrosion protection [62,101]. One example of the Li-based conversion layer structure grown on the aluminium matrix is shown in Fig. 3, which includes a distinct inner dense layer (red arrow) and a columnar outer layer (blue arrow). Li ions distribute within the entire inner and outer layer (shown in Fig. 4), and the inner layer mainly consists of Li-pseudoboehmite. It has been reported that amorphous aluminium hydroxide can serve as Li-sorbents to collect Li from brine lakes, and a low Li content limits an effective transformation of amorphous aluminium hydroxide into crystalline Li/Al LDH [102–104].

Recent studies conducted by Visser et al. [62] and Kosari et al. [101] discussed the conversion bath containing Li_2CO_3 and NaCl to establish a detailed Li-based conversion layer formation model. While the Li-based conversion layer immersed in a lower concentration Li_2CO_3 (0.01 M) failed to provide similar corrosion protection compared to that formed at higher concentrations, the reported conversion layer formation mechanism remained the same. The formation model that was established is provided in Fig. 5. The existence of three types of IMPs (S-, θ- and constituent phases) is considered here. The entire formation process discussed in these works can be divided into five stages: After exposure to the aggressive conversion bath (pH $\geq$ 10), the air-formed oxide layer experiences a fast dissolution followed by the dissolution of the aluminium matrix and the dealloying of IMPs, most notably the electrochemically active S-phase (Stage I) [62,101]. This morphological change is reflected by a sharp drop in the OCP. The initial dissolution rate might differ between intermetallic particles and the Al matrix and even vary within the aluminium matrix [72]. This phenomenon is caused by the heterogeneous compositional distribution across the aluminium alloy surface. During stage II, the Al matrix still undergoes massive dissolution and the S-phase first exhibits a fast dealloying which

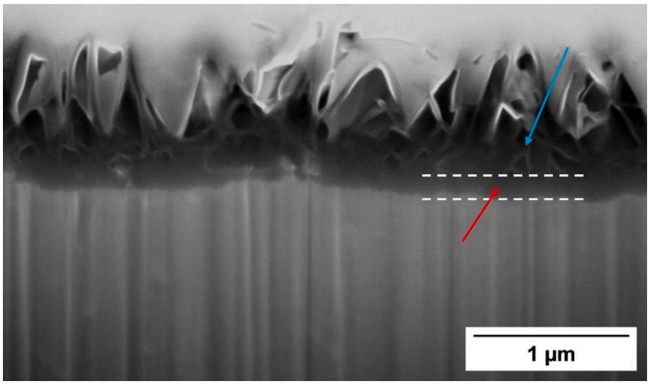

Fig. 3. Cross-sectional image of the Li-based conversion layer on AA2024-T3. The panel (Exposed surface: 10 mm in diameter) was immersed in a 0.01 M Li_2CO_3 and 0.01 M NaCl solution (volume: 0.321 mL) for a duration of 7 h. The red arrow refers to the inner dense layer while the blue arrow indicates the outer columnar layer. (For interpretation of the references to colour in this figure legend, the reader is referred to the web version of this article.)

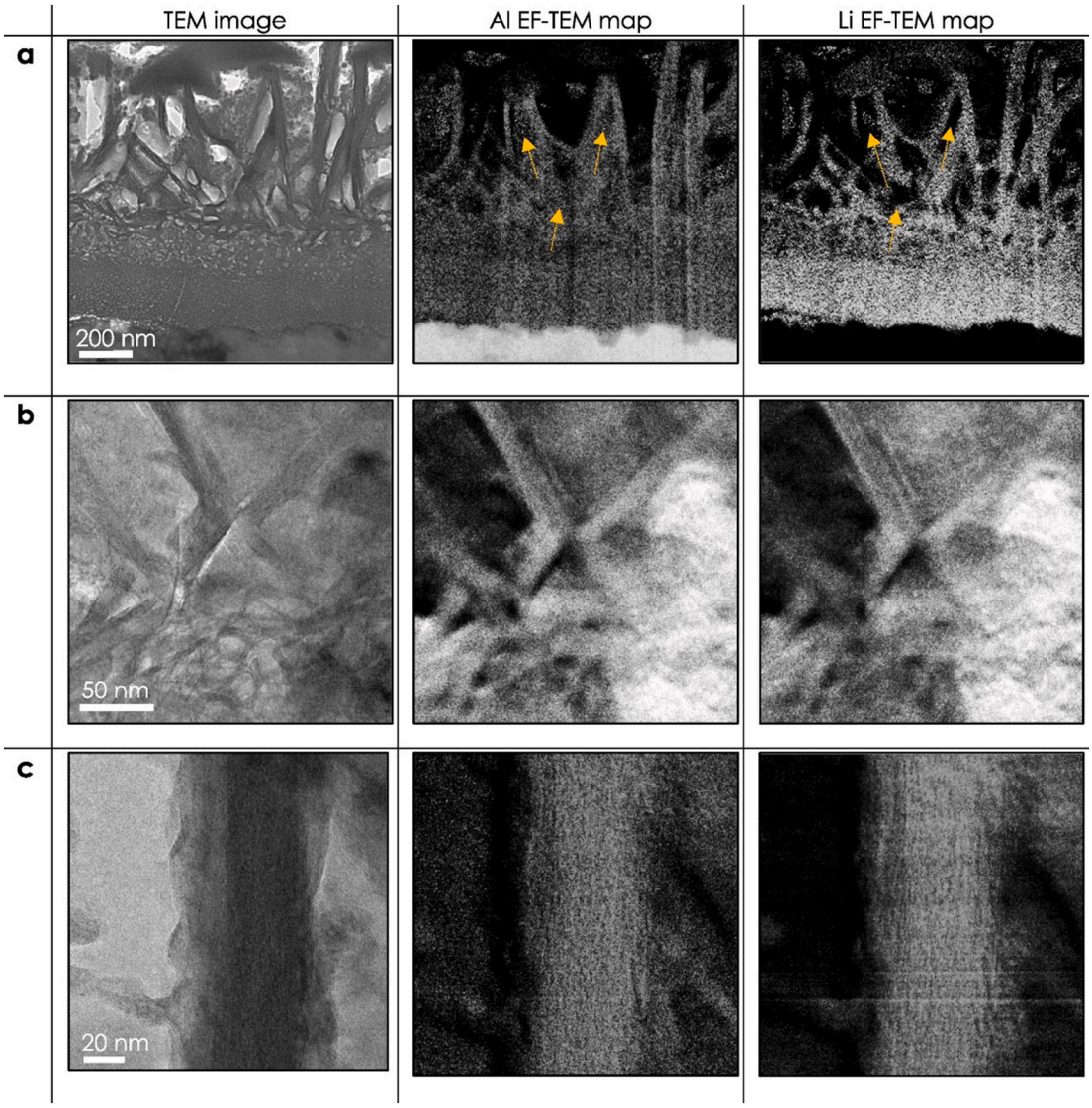

Fig. 4. Bright field transmission electron microscopy (TEM) images and the corresponding energy filtered (EF)-TEM maps of Al and Li distribution of the Li-based conversion coating from an Li leaching organic coating sample with defect after 168 h neutral salt spray: (a) the entire layer formed in the peripheral region; the yellow arrows indicate Li-free region, (b) at columnar layer/porous layer interface and (c) a single columnar LDH top layer [105]. (For interpretation of the references to colour in this figure legend, the reader is referred to the web version of this article.)

results in surface enrichment of Cu, leading to the transition of the S-phase from an anodic to cathodic nature and accompanied by the appearance of trenches around its perimeter [101]. The Cu enrichment drives the OCP in the positive direction. Meanwhile, the crystalline Li/Al LDH is not formed until the concentration of aluminate ions at the alloy/solution interface reaches a supersaturation threshold concentration. Considering the high pH at the alloy/solution interface during the initial stages (I and II), aluminate is more chemically stable in the medium. The decease of pH and gradual saturation of aluminate over time slow down the dissolution kinetics of the aluminium alloy surface, especially when the dissolution front penetrates deeper, thus generating a larger diffusion distance [72]. At stage III, the columnar Li/Al LDH appears when the local concentration of aluminate reaches supersaturation [72,101]. Nevertheless, different regions attain aluminate supersaturation asynchronously. Areas with a higher aluminium dissolution rate reach aluminate supersaturation earlier. For example, the appearance of the top columnar layer over the S-phase on AA2024-T3 precedes that over adjacent aluminium matrix (this even already occurs at the end of stage II), whereas the relatively electrochemically stable θ-phase and constituent phase do not show evidence of the formation of a columnar layer earlier than the aluminium matrix [101]. The aluminium source for the S-phase originates from the dealloying of its aluminium content. The θ-phase and constituent phase both experience a slight dealloying, but this limited dealloying cannot provide sufficient aluminium to support the precipitation of crystal Li/Al LDH. In addition, the newly formed Li/Al LDH may dissolve again at the location closer to the solution side [72]. At stage IV, the size and number of Li/Al LDH plates both increase over the aluminium matrix as well as over the S-phase. Meanwhile, the Li/Al LDH starts to appear over the θ-phase and constituent phase. This local supersaturation is mainly caused by the lateral propagation of the aluminate ions from the adjacent aluminium matrix. Finally, at stage V, the densification of the Li/Al LDH slows down the diffusion process between the metal/LDH interface and the liquid environment, which results in a lower pH at the metal/LDH interface. A lower pH and also a lower supply of Li ions enables the densification and thickening of the inner protective layer. Simultaneously, the top LDH layer exhibits sustained growth via the precipitation of lithium-containing species, leading to the coarsening of its columnar structure. It should be noted that the inner dense layer is absent above S-, θ-, and constituent phases due to an insufficient supply of dissolved aluminium, which may create weak

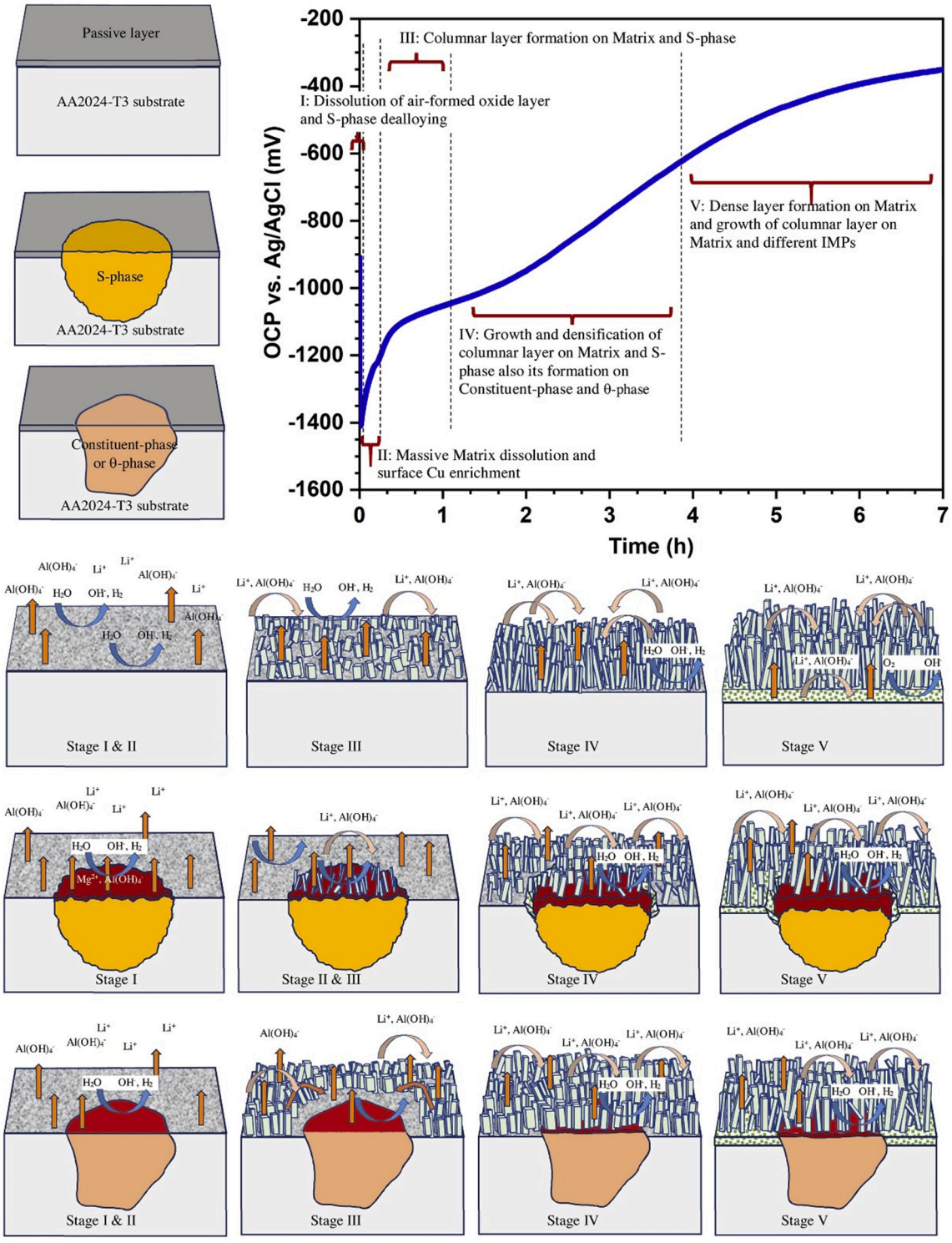

Fig. 5. Schematic overview of the formation mechanism of the Li-conversion layer on AA2024-T3. The conversion layer formation stages are linked to the OCP. This schematic depicts the local morphological variation of the layer formation at the alloy matrix and IMPs [101].

spots in the protective layer. Upon reaching Stage V, the system attains a state of pseudo-stability, reflected by a plateau in the OCP curve, which is attributed to the passivation effect induced by the mature Li-based conversion layer. Currently, detailed conversion layer formation mechanism analysis is only performed on AA2024-T3. While a similar conversion layer growth mechanism is expected on other commercial aluminium alloys, its investigations are still pending. This is due to the presence of compositionally varying IMPs in various aluminium alloys, potentially giving rise to disparate effects on the local development of the Li-based conversion layer especially at IMPs.

Usually, for bulk specimens the conversion layer consists of a bilayer structure, whereas ultra-thin samples prepared for liquid-phase TEM (LP-TEM) characterization contain an extra middle porous structure [72,101]. It has been reported that the porous structure observed for layers formed from the organic coating system consists of a mixture of Li-pseudoboehmite and Li/Al LDH [105]. This difference might be

attributed to variations in local liquid environments, which is caused by the different ratio of the exposed surface to the volume of the electrolyte. For the bulk material, a higher surface-to-volume ratio shows a faster pH decrease during the conversion layer growth period since the hydroxyl ions are consumed continuously. A moderate pH is beneficial for the stability of the top columnar layer as well as the formation of the inner dense layer [72]. This explains why the transitional middle porous layer between the outer crystalline LDH layer and the inner dense layer is not observed to grow over the bulk sample, since the local pH close to the conversion layer is less aggressive for the case of bulk samples. In addition, the top LDH layer is very porous and the protective behaviour is dependent on the thickness of the inner barrier layer at the interface between the metal and the protective coating [106].

Based on the formation mechanism mentioned above, several influential conversion bath factors on the Li-based conversion layer growth are discussed here. Local supersaturation of the aluminate ions necessitates the growth of the Li-based conversion layer. Therefore, adding aluminate ions (by dissolution of pure aluminium in the conversion bath or the addition of aluminate salts) into the conversion bath containing lithium salts enables a better performance in salt spray tests [49]. Another finding that supports the importance of the supersaturation of aluminate ions is that the conversion layer formation is very sensitive to the volume of the conversion electrolyte (containing 0.01 M Li_2CO_3) [72]. A small volume of electrolyte generates a conversion layer providing a higher corrosion resistance. The experimental results from Kosari et al. [101] show that it takes several hundreds of seconds to reach local supersaturation, which implies that a certain amount of aluminate ions may diffuse away from the alloy surface and does not contribute to the formation of the Li/Al LDH. A smaller liquid volume is beneficial to restrict the diffusion of aluminate ions. Therefore, it appears that shortening the duration for realizing the supersaturation of aluminate ions favours a high-quality conversion layer formation. Alloying elements also play an important role in the quality of the Li-based conversion layer. Up to now, only the effect of Cu was reported by Buchheit et al., which shows that its presence is detrimental for the quality of the Li-based conversion layer. Aluminium alloy surfaces enriched with Cu generate a thinner conversion layer as compared to Cu-free alloy surfaces [52]. Moreover, a freshly-formed Li-based conversion layer, generated in a conversion bath at pH 11.5, on AA2024-T3 showed a much higher corrosion resistance after immediate re-immersion in a high pH (approximately 13.5) conversion bath containing Li_2CO_3, LiOH, and $NaAlO_2$. This is due to the removal of the surface enriched Cu when exposed to a high pH solution containing carbonate ions. A possible reason to explain the unfavourable effect of Cu is that it acts as a noble element. Cu enrichment over the alloy surface during the conversion layer formation drastically increases the OCP which impedes the hydrogen evolution for a short period. Meanwhile, a fast dissolution of aluminium is necessary to provide sufficient aluminate ions in order to reach the supersaturation state before the formation of the conversion layer. Therefore, fast cathodic reactions are very important for the counterbalance of the rapid anodic dissolution. Oxygen reduction is insufficient to support a large cathodic current, due to its limited supply by the diffusion through air, which hinders the continuous supply of aluminate ions. This explanation also corresponds to the finding that the conversion bath added with oxidizing agents is favourable to enhance the corrosion resistance of the conversion layer, since these oxidants consume electrons which promotes the aluminium dissolution. The distribution of Cu throughout the entire Li-based conversion layer has been reported before [72], but its influence on the structural stability of the Li-based conversion layer still requires further investigation. Cu aside, the effects of other noble alloying elements still remain uncertain, which necessitates additional study.

Except for a qualified stand-alone corrosion protection capacity provided by the chemical conversion coating, another criterion to evaluate Li-based conversion layers is their interfacial bonding to organic coatings, as well as the overall corrosion protection within a coating system. Some early work performed by Buchheit et al. [53] revealed that Li-based conversion layers prepared by nine different conversion baths showed favourable stand-alone performance compared to bare AA2024-T3, but worse behaviour for an organic coating system, i.e. a Li-based conversion layer covered by commercial primers compared to the non-conversion coated but primed sample. One possible reason lies in the reversibility of the intercalation of the conversion layer formation process. The liberation of ions during the de-intercalation beneath the primer establishes an osmotic gradient, thereby promoting the ingress of water from the external environment.

3. Li-based inhibitor coating technology and performance

Apart from the studies on the Li-based chemical conversion layers, the exploration of Li-containing species as leachable corrosion inhibitors that can be incorporated into organic coatings makes notable progress. The incorporation of Li salts in a coating was based on the previous studies of the Li-based chemical conversion coating [47–51,55]. The hypothesis whether it was possible to generate a protective film in a defect directly from a coating was postulated based on this prior work. In 2010, the utilization of Li salts loaded in a coating as a replacement for $SrCrO_4$ primers was first reported by Visser and Hayes [107], revealing fast, effective and irreversible corrosion protection after a neutral salt spray test exposure for 168 h [39,108]. The primer was a fully formulated polyurethane primer system consisting of the pigment TiO_2 and extenders MgO and $BaSO_4$ and the inhibitor, Li_2CO_3. AA2024-T3 panels were anodized in tartaric-sulfuric acid according to aerospace requirements (AIPI 02-01-003) before spraying the Li-containing primer. The Li-containing primer has been proven to provide comparable corrosion protection as traditional hexavalent-chromium-containing organic coatings [42]. Although Li salts may not be the candidate that offers the highest intrinsic corrosion inhibition properties as compared to certain organic inhibitors like benzotriazole (BTA) [109] and 2-mercaptobenzothiazole (2-MBT) [110] when exposed to an inhibitor-containing electrolyte, they do show the highest remaining inhibition, i.e. irreversibility, when subsequently exposed to a non-inhibitor containing corrosive solution [108]. This irreversibility of corrosion inhibition is an important factor when selecting favourable candidates, especially for long-term corrosion protection after the depletion of loaded inhibitors inside the coating matrix [108]. The results reveal that the Li-based protective layer formed inside a scratch still provides constant corrosion protection even after a re-immersion of 5 days in a Li-free solution, whereas BTA and 2-MBT both present a reversible nature, resulting in severe corrosion of the aluminium alloy in case of a diminishing supply of inhibitors.

Assessment of the protective efficiency of organic coatings loaded with Li salts is commonly achieved through the introduction of an artificial scratch (usually 1 mm in width) in these coatings, and comparing its corrosion performance to reference clear coating systems, i.e. in the absence of inhibitors [39–43]. Optical images of different samples are shown in Fig. 6. After a 168 h salt spray exposure, the scribed reference samples showed the presence of a large number of corrosion products (Fig. 6b). Localized corrosion such as pitting and intergranular corrosion is observed as well [39]. By contrast, the specimen with Li inhibitors presented negligible corrosion damage (Fig. 6c, d) and the substrate of the scribe was shown to be covered with a multi-layered structure [40,111]. Fig. 7 shows a representative structure of the Li-based conversion layer from the artificial defect of a coating sample, which includes a top columnar layer, a porous middle layer, and an inner dense layer. A detailed discussion of this protective coating formation at the coating defect will be presented later.

A quantitative analysis of the corrosion resistance regarding the film generated within the scribed region after the salt spray test has been performed through various electrochemical characterization techniques [40,42,63,64,108,112]. EIS measurements are often performed to characterize the corrosion protective properties of the formed

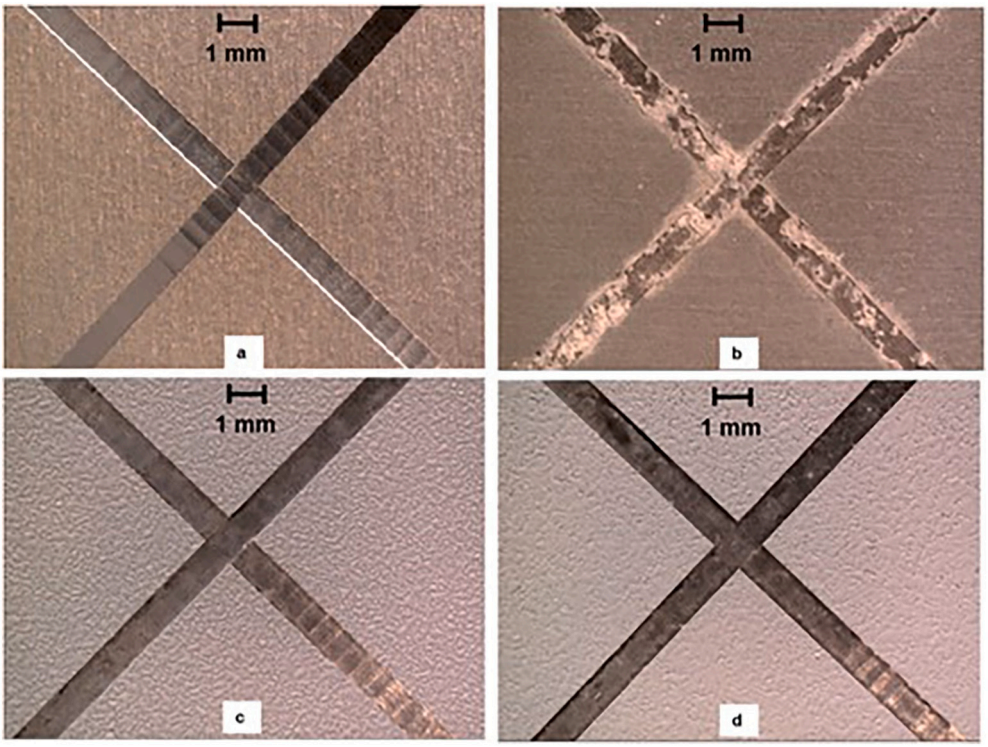

Fig. 6. Optical images of coated AA2024-T3 samples with artificial scribes before and after 168 h neutral salt spray exposure (a) unexposed (b) without inhibitor, (c) lithium carbonate loaded and (d) lithium oxalate loaded coating. Reprinted from [39] with permission from the Royal Society of Chemistry.

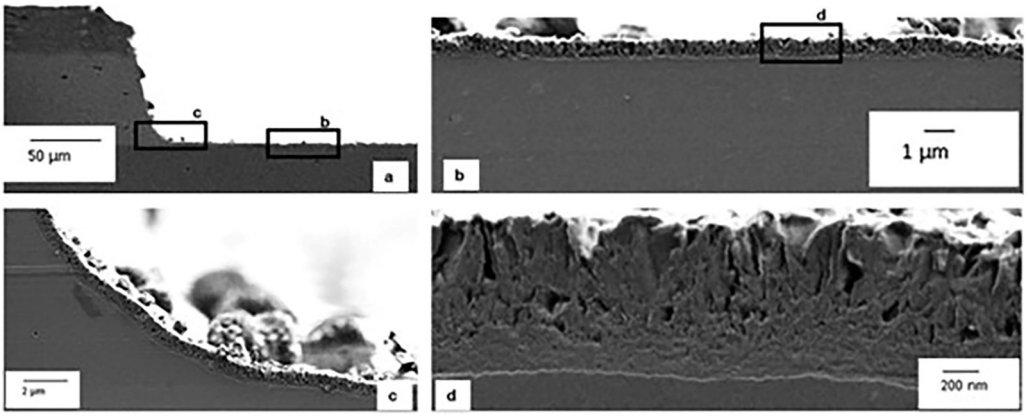

Fig. 7. SEM cross-sectional views of protective layers generated from a lithium carbonate loaded coating after 168 h neutral salt spray exposure (a) scribed area, (b) middle region of the scribe, (c) curved location of the bottom of the scribe, (d) detailed multi-layered morphology of the conversion layer. Reprinted from [39] with permission from the Royal Society of Chemistry.

conversion layers [40,108]. It has been reported that the low-frequency impedance modulus values of a Li_2CO_3 containing coating system are about one order of magnitude higher as compared to that of a reference Li-salt free system, and that the low-frequency impedance modulus of a Li-oxalate-loaded sample is about two times higher than that of a Li_2CO_3-containing sample [40,42,106]. Moreover, higher impedance modulus values in the medium frequency range (1–100 Hz) indicate the formation of a protective film as well. The increased and broadened phase angle values of the lithium-loaded specimens after 168 h salt spray exposure observed in the corresponding Bode plots suggest the formation of a thicker and more stable (oxide) layer in the defect area. Using microcapillary cell techniques [113,114], potentiodynamic polarization measurements can be performed at a small exposed surface in the scribed area after a 168 h salt spray exposure. Compared to the unexposed samples, the corrosion current for samples loaded with Li salts reduces almost one order of magnitude and the corresponding pitting potential drastically rises up to >1500 mV vs. AgCl, 3 M KCl [42]. It should be noted however that the results present a scattered distribution due to the heterogeneous nature of the coating layer and substrate, as a result of different local chemical conditions during its formation. A duration of 2 h of exposure to a salt spray test has been documented to be a noteworthy improvement of the impedance modulus value in the low- and mid-frequency range since the protective film, especially the inner dense layer, starts to cover the exposed surface effectively [106]. Furthermore, an investigation into the efficacy of a Li_2CO_3-loaded coating has revealed an inhibition efficiency of approximately 80 % within 2 h of exposure, which subsequently increases to an impressive 95 % after 48 h. Remarkably, this heightened level of inhibition remains relatively stable, even after prolonged exposure times.

Up to now, most measurements and analysis on coating samples were

focused on AA2024-T3. For other aluminium alloys, the evaluation of the corrosion protection of Li salts leaching organic coating was performed on AA7075, AA5083, and AA6014 so far [111]. Fig. 8 shows the fitting results from EIS measurements for samples with artificial scratches before and after the 168 h neutral salt spray test. R_{oxide} and C_{oxide} indicate the resistance and capacitance values of the oxide layer, respectively, which refers to the native oxide layer for the case without inhibitors, and the inner dense layer for the samples loaded with inhibitors. R_{pol} and C_{dl} represent the polarization resistance and the double layer capacitance at the metal/oxide interface, respectively. It is obvious that the trend of increased resistances and decreased capacitances is identical for AA2024, AA7075, and AA5083, which is consistent with the presence of the Li-containing protective layer in the defect area. AA2024 still presents the lowest corrosion resistance but the highest inhibiting effect is realized in the presence of Li_2CO_3. The distinct behaviour of AA6014 is attributed to its intrinsic self-passivating property. These tests indicate that the active protective behaviour of Li leaching organic coatings is to a certain extent relatively independent on the metallurgy nature and complexity of the aluminium alloys.

4. Li-based inhibitor action in coating defects

It is important to investigate the diffusion process from the coating matrix to and within a coating defect area. A crucial parameter is the

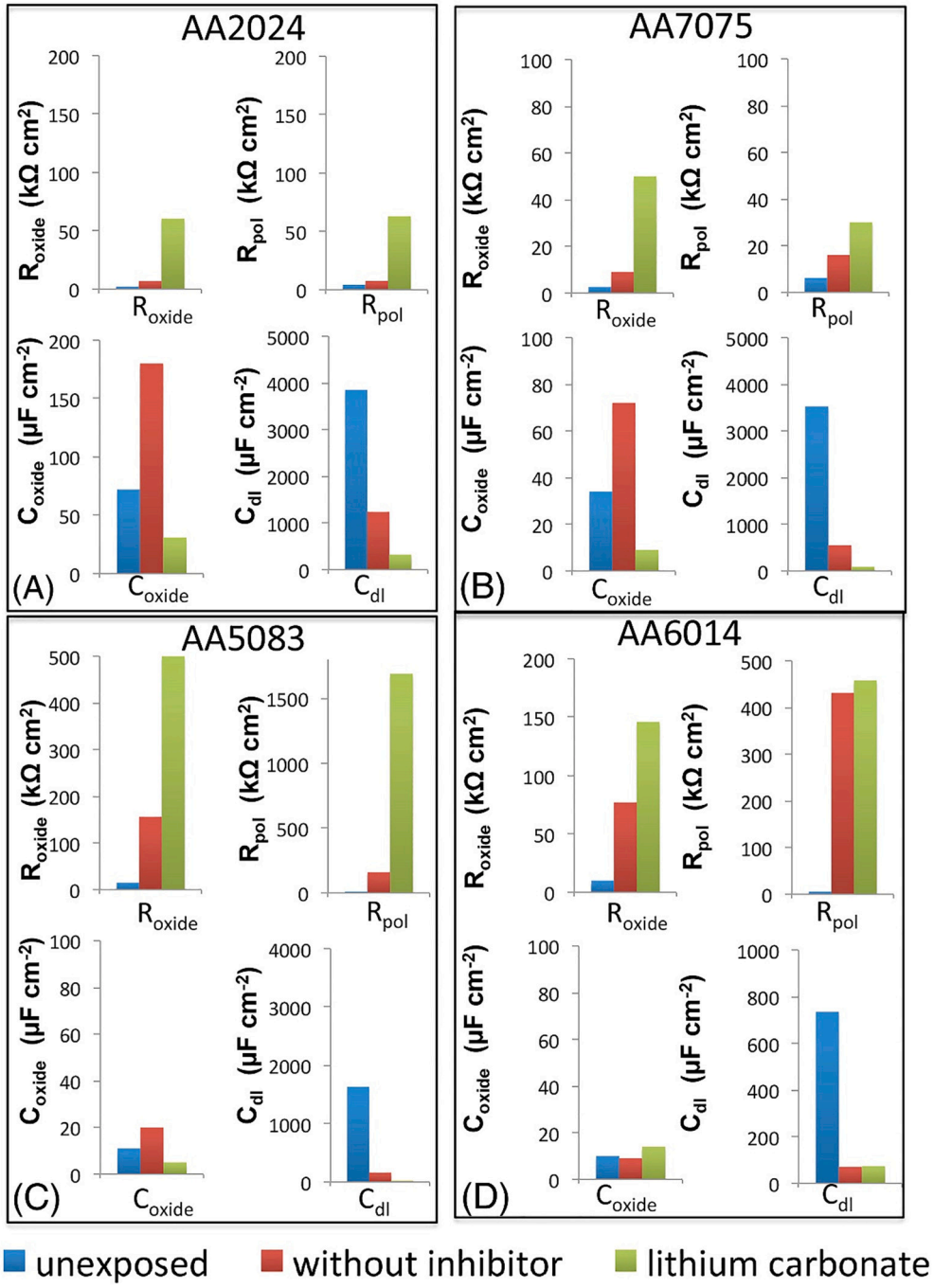

Fig. 8. Results of the electrochemical parameters including oxide resistance (R_{oxide}), polarization resistance (R_{pol}), oxide capacitance (C_{oxide}), and double layer capacitance (C_{dl}) inside the artificial defects of different aluminium alloys covered by coatings loaded with and without Li_2CO_3 before and after neutral salt spray test: A, AA2024; B, AA7075; C, AA5083; and D, AA6014 [111].

effective coverage distance of the released inhibitor against corrosion inside a defect area, commonly referred to as chemical throwing power [115,116]. This process entails a transport with stochastic nature, accelerated by the concentration gradient of inhibitors, facilitating the mobility of inhibitors from regions enriched with inhibitors to sites that require protection [117]. Owing to the fast initial dissolution of lithium salts, a critical local concentration is achieved at the edge region of the scribe, which guarantees a considerable throwing distance, and hence a considerable scribe coverage. It has been reported that even a relatively low lithium salt load (e.g., 2.5 % pigment volume concentration (PVC)) can already effectively protect the exposed scribed area for up to a width of 6 mm [66]. The released Li ions can relatively uniformly cover the entire defective area with a width of 1 mm within 15 min. However, due to variations in local conditions such as pH and local concentrations of lithium ions, distinctly different morphologies and chemical compositions are generated at different locations within the coating defect [40].

Compared to the conversion layer formation process in the conversion bath, the growth stages of the Li-based protective layer are much more complex due to the varying leaching kinetics of the Li salts from the coating matrix [118]. In general, the local pH and the concentration of Li ions gradually increase over time in the beginning. This trend initially occurs adjacent to the cut edge and subsequently gradually propagates towards the centre of the scribe. A detailed schematic overview showing the formation of the Li-based protective layer inside the artificial scratch over time can be seen in Fig. 9. This formation process inside a defect can be divided into five stages [67]. Initially (stage I), rapid leaching of Li salts enables a sharp increase in pH due to the hydrolysis of carbonate anions. Although the local pH was reported to be lower than that of the conversion bath [43], this is sufficient to cause thinning of the air-formed aluminium oxide layer [119]. Simultaneously, the unprotected surface area is exposed to the aggressive chloride-containing environment. At stage II, anodic dissolution of the alloy surface is triggered and simultaneously an aluminium hydroxide gel forms, which is thicker than that formed in the conversion bath due to a milder alkaline condition [120]. This gel layer will gradually expand from the edge to the central area and transform into pseudoboehmite. Pseudoboehmite exposed to a Li-containing solution in turn transforms to Li-pseudoboehmite due to the intercalation of Li ions [43]. At stage III, Li-pseudoboehmite gradually develops towards the central area and in the meantime the concentration of Li salts reaches a certain threshold near the edge area, leading to the transformation of Li-pseudoboehmite into a columnar Li/Al LDH structure, since LDH is more stable in a more alkaline (pH $\geq$ 10) environment [20,121,122]. With prolonged exposure time in a salty electrolyte, a continuous rise in the concentration of Li species within the central region of the scribe is reached. This elevated concentration of Li ions facilitates the growth of LDH within the central area of the scribe (stage IV). Finally, at stage V, a columnar LDH layer progressively expands laterally at the surface until a complete coverage of the scribe by LDH is achieved. Furthermore, differently to the bilayer structure as generated in the conversion bath, the Li-based protective layer inside a scratch comprises of three distinct layers: an inner dense layer, a middle porous layer and an outer columnar layer [26]. As mentioned in Section 2, the middle porous layer is in fact a transition zone that gradually evolves from Li-pseudoboehmite to Li/Al LDH. The ratio between these three layers also varies locally: areas close to the cut edge contain a higher ratio of columnar Li/LDH, whereas regions around the central area are mostly composed of Li-pseudoboehmite [39]. At last, pseudoboehmite is expected to be the dominant composition in the central region when the diffusion distance is large enough, e.g., for a scribe width of 6 mm.

5. Li-based inhibitor mobility in and leaching from coatings

Understanding how inorganic inhibitor particles are distributed within a coating microstructure is helpful for understanding their leaching behaviour and for optimizing the design of future coating systems [123]. Previous studies on the leaching behaviour of hexavalent-chromium-based inhibitors revealed that inhibitor particles aggregate in clusters within the polymeric matrix and that the leaching of corrosion occurs through the dissolution of interconnected soluble particles and ion mobility within such media does not follow pure Fickian diffusion. The voids resulting from dissolved chromate particles can form transport paths within the coating in combination with the low density areas, facilitating the release of inhibitors and the ingress of electrolyte [123,124]. These pathways possess significance due to the large size of the chromium ion, thereby precluding diffusion through the epoxy but permitting transport exclusively through channels formed by the dissolution of chromium-based particles [125].

The assessment of Li distributions in organic coatings poses challenges in electron beam spectroscopy owing to the low energy Li K-alpha line position and lack of detector sensitivity [67]. As a result, other techniques have been explored to determine the Li distribution within primers. Alpha-Particle Induced Gamma-ray Emission (PIGE) mapping, for example, was used to map the Li distribution within the polyurethane primer coating. This study showed that the observed Li-containing particles were often connected by small channels in the polyurethane matrix and around the individual particles [126].

The depletion of Li-containing particles from the coating matrix is a complex process in which inorganic phases and mechanical stress are reported to be involved [69,118]. First, the leaching of lithium salts from an organic coating system without a topcoat under neutral salt spray test exposure will be discussed. The release properties of Li ions from organic

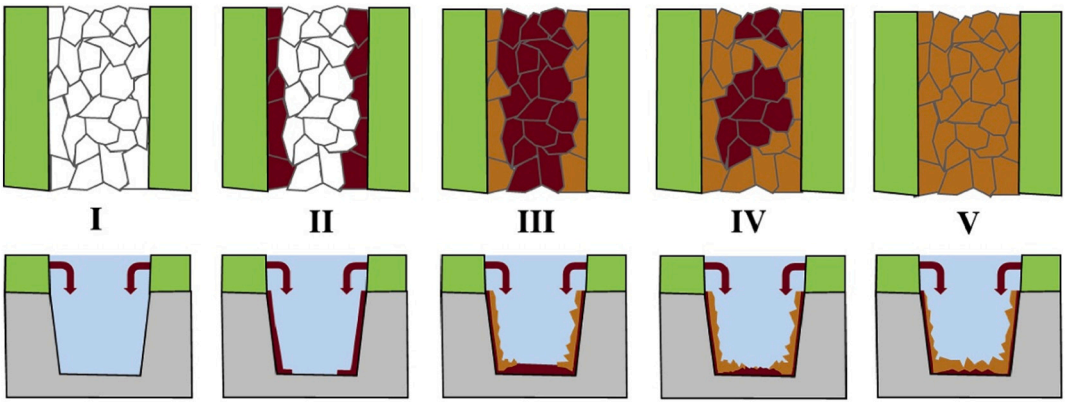

Fig. 9. Schematic representation of the growth stages of the protective layer inside a scratch (1 mm in width) of an organic coating under exposure of a neutral salt spray. The dark red and brown colours (Stages II to V) indicate Li-pseudoboehmite and Li/Al LDH, respectively. Reprinted from [67] with permission from Elsevier. (For interpretation of the references to colour in this figure legend, the reader is referred to the web version of this article.)

coatings depend on the solubility of different Li salts, the loading of Li salts in the primer matrix, and the microstructure of the matrix [66,127]. Water uptake and leaching kinetics of inhibitors for inhibited primers are one of the important subjects of previous studies [128–130]. Upon exposure to a liquid environment, water uptake occurs quickly within the first few hours through the free volume of the polymer [128,129,131–133]. It has been reported that the characteristic size of the free volume of polyurethane is approximately 3.7 Å, which is larger than the diameter of a water molecule at 3.0 Å [134]. In addition, the process of ion uptake generally exhibits a deceleration, which particularly counts for chloride, typically occurring at a rate approximately two orders of magnitude lower as compared to the rate of water diffusion [132]. Therefore, water uptake is the main factor which is influential for the behaviour of the primer at an early-stage. Subsequently, some absorbed water will reach the interface between the polymer matrix and the particles underneath the top area of the primer, where hydrolysis reactions will occur. The presence of water results in the dissolution of Li_2CO_3 particles and slight dissolution of MgO particles. Later, the local electrolyte develops surrounding the Li_2CO_3 particles, generating a high concentration and thus absorbing water from the nearby primer matrix due to osmotic effects [132]. The origin of the induced internal stress is attributed to the difference between hydrostatic and osmotic pressures, which may lead to local rupture and delamination around the Li_2CO_3 particles. The creation of those channels results in a fractal network that functions as a porous medium, leading to a deeper penetration towards the metal/primer interface after longer exposure times [69]. Once these channels are connected to the external surface, the electrolyte with dissolved Li_2CO_3 will be released or at least redistributed within the network.

Parallel to the process of water uptake, the formation of a uniform depletion zone of Li_2CO_3 occurs rapidly in the upper part of the primer, which can be seen in Fig. 10 [69]. Energy dispersive X-ray spectroscopy (EDS) was used to characterize the distribution of different types of particles under various exposure times [69]. The elemental colour indications are shown in the legend positioned at the bottom of each map (Li_2CO_3 particles in red colour). Only Li_2CO_3 particles directly

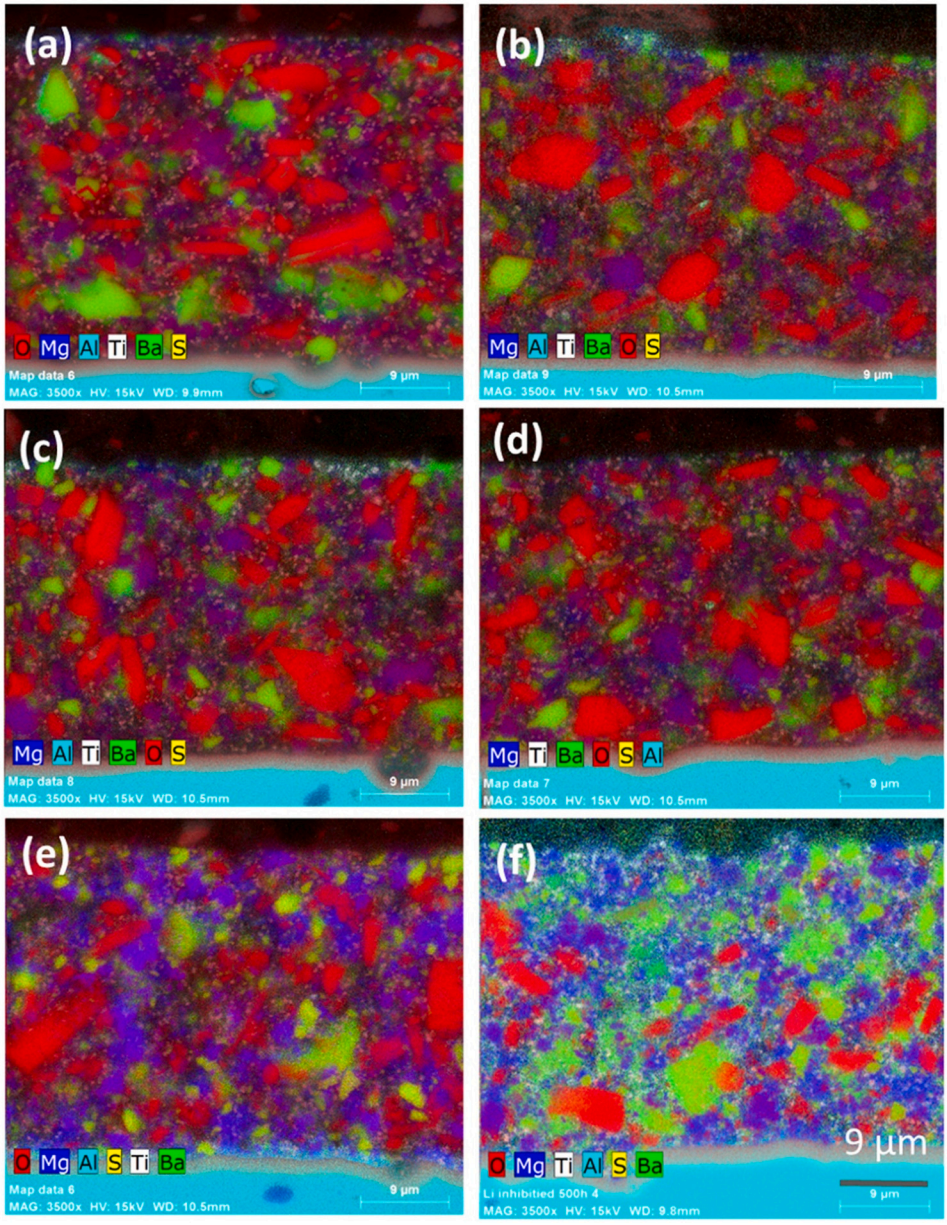

Fig. 10. EDS maps of leaching from a Li_2CO_3 containing primer at different exposure times under neutral salt spray. (a) 0 h, (b), 8 h, (c) 48 h, (d), 96 h, (e) 168 h and (f) 500 h. Reprinted from [69] with permission from Elsevier.

connected to the external electrolyte dissolve after short exposure times (<8 h). The dissolution of Li_2CO_3 particles positioned deeper (occurring after exposure time longer than 96 h) are related to the delamination/dissolution of Li_2CO_3 particles which will be discussed later. This fast initial dissolution of Li_2CO_3 is also reflected in the high early-stage Li-ion release rate detected by inductively coupled plasma atomic emission spectroscopy (ICP-AES) [69]. Following the initial fast release of Li, Mg and, to a lesser extent, Ba are released as well. The initially high release of Li rapidly drops to a low ongoing release, which may result from the exhaustion of the leachable Li_2CO_3 particles that are connected to the external surface [69]. Subsequently, localized depletion of Li_2CO_3 extends deeper into the coating underneath this zone, indicating the involvement of the clusters of Li_2CO_3 particles in the release process [118]. This gradual dissolution does not necessarily propagate as a distinct "front" through the cluster, where particles closer to the surface must fully dissolve before particles further away from the surface can dissolve. Instead, it occurs through the concurrent dissolution of particles at varying depths within the clusters, which is governed by the transport of inhibitor within the cluster/void channels through the electrolyte.

Exterior surfaces and some internal structural areas of aircraft are coated with chemical resistant topcoats [17]. This will influence the water uptake of the coating and the inhibitor leaching kinetics. External mechanical forces may cause crevices, cracks or scratches in the coating, causing the exposure of the Li-containing primer and the metallic substrate to the external environment. Therefore, it is meaningful to discuss the leaching behaviour into a defect from the cut edge of the Li-containing primer underneath a topcoat. Unlike the leaching from the as-primed surface, here only a small cross section of the primer is exposed to the liquid environment, i.e., the scribe edge. However, hydration process, dissolution reactions of inorganic particles, and the generation of networks are still involved in this case. A summarizing mechanistic overview of samples after a salt spray test can be seen in Fig. 11 [70]. Before exposure, the scribe damage influences the coating microstructure 20 to 25 μm away from the scribe edge, leading to the deformation of the primer and detachment around Li_2CO_3 (red colour) and $BaSO_4$ (yellow colour) particles. This detachment creates a loose structure close to the cut edge and provides networks for relatively fast early-stage ingress of electrolyte. After a sufficiently long exposure time (500 h), the depletion of inorganic particles (mainly Li_2CO_3, MgO and $BaSO_4$) at the area affected by deformation occurs, whereas the particles further away from the cut edge show a partial dissolution which is associated with the propagation of the channels within the primer. After an exposure of 48 h, dissolution sites appear, surrounding Li_2CO_3 particles (red arrows in the middle figures) at a distance of over 2000 μm away from the scribe, as well as a small number of detachment at the primer/Li_2CO_3 interface (pink arrows in the middle figures). A limited dissolution of $BaSO_4$ is also observed and marked by yellow arrows. No cracks in the primer matrix are observed. After an exposure duration of 168 h, more dissolution and detachment sites around and in Li_2CO_3 particles, as well as the dissolution sites of $BaSO_4$ particles, are observed. However, the number of detachment sites increases, indicating that the diffusion networks extend wider and deeper into the primer matrix. In addition, cracks are present inside the primer, extending from the dissolution or detachment sites. The partial dissolution and the appearance of cracks are related to the uptake of water. Considering the diffusion distance, water ingress through the topcoat is more dominant for the area relatively far away from the scribe. The osmotic and swelling pressures caused by the water uptake generates inner stresses, which makes certain sites more susceptible to mechanical degradation.

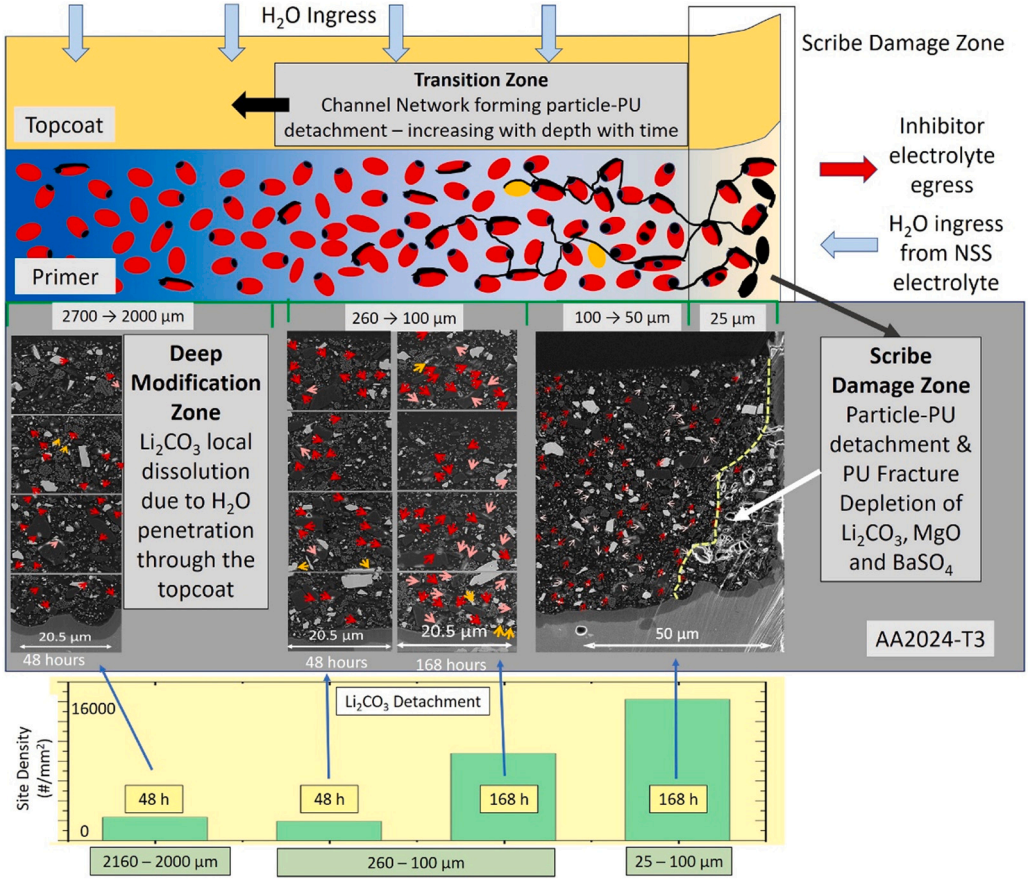

Fig. 11. Schematic representation of the leaching characteristics of an AA204-T3 substrate including primer and topcoat. Reprinted from [70] with permission from Elsevier.

These results indicate that besides the inhibitor component, also other particles with non-inhibiting functionalities are involved in the process of inhibitor release. For this reason, tailoring the composition of the organic coating system is of vital importance to optimize the leaching behaviour of loaded inhibitors [135]. In the context of organic coatings relying on the release of inhibitors by the leaching process, the optimization of the transport of inhibitor ions constitutes a pivotal objective. For example, the shape, size and distribution of the inhibitor clusters play an important role in the leaching kinetics [136], and these parameters are strongly influenced by the PVC and other non-inhibitive compounds. Relevant studies focussing on the optimization of the coating microstructure design are still relatively limited for Li leaching coatings.

6. Conclusions and outlook

Li-based inhibition technology has demonstrated its performance potential for the replacement of conventional chromate inhibitors for both conversion surface treatment as well as leachable inhibitors from active protective coatings for aluminium alloys. In addition to their significant corrosion protection performance, Li salts also have the advantages of being environmentally friendly and cost-effective, as well as offering irreversible long-term corrosion protection.

Nonetheless, current studies indicate that Li-based conversion treatments still require a longer process time to reach comparable corrosion protection as compared to chromate-based conversion treatments. This potentially hinders its industrial use. Feasible strategies should be developed in order to modify the composition of the conversion bath in order to shorten the conversion treatment while maintaining or even improving its corrosion protection performance. Detailed studies on the influence of alloying elements from different commercial aluminium alloys, the extra additives, especially those components which can improve the quality of the conversion layer such as oxidants and aluminate salts, still remain to be performed.

For an organic coating system, the morphological layer evolution at a coating defect is different to that on aluminium alloy panels exposed to bulk electrolytes which are characterized by relatively stable pH values and Li concentrations. In the bulk electrolyte case, firstly a Li/Al LDH is formed which is more stable in a highly alkaline solution, followed by the generation of a dense inner layer. The conversion coating approach is more based on the precipitation of LDH in a super saturated solution. By contrast, in the case of the organic coating system, the lower initial pH and Li concentration initially triggers the anodic dissolution of the exposed alloy surface, leading to the formation of a dense Li-pseudoboehmite. With an increase in the concentration of Li salts and pH, Li-pseudoboehmite is partially converted into Li/Al layered double hydroxide (LDH). Current studies on the elucidation of the protective layer formation mechanism for organic coating conditions are mainly performed using Li_2CO_3 and NaCl, and mostly limited to the case of AA2024-T3. Therefore, the protective layer formation mechanism under a more complex environment (e.g., the influence of other common dynamic atmospheric corrosion conditions) and other aluminium alloys still need more investigation in the future. In addition, understanding the stability of the protective layer and how this can be optimized is also a relevant subject of further study.

The microstructure of the coating matrix plays a vital role in the leaching behaviour of inhibitors. Particles inside the primer matrix without inhibition abilities influence the formation of distinct inhibitor delivery pathways. Therefore, a more profound understanding of the inner transportation networks is necessary for an optimization of the coating design to improve the active corrosion protection efficiency. Moreover, the porous Li/Al LDH structure contributes little to the corrosion protection. This effect can be utilized by chemical conversion treatments since the chemistry of the conversion bath and post-treatment can be controlled. On the contrary, for the case of the Li salts leaching organic coating, it remains challenging to control the top LDH layer. This might be an interesting topic for future research where a more profound understanding and control of leaching kinetics are addressed.

CRediT authorship contribution statement

Ziyu Li: Conceptualization, Formal analysis, Investigation, Writing – original draft. **Peter Visser:** Writing – review & editing. **Anthony E. Hughes:** Writing – review & editing. **Axel Homborg:** Supervision, Writing – review & editing. **Yaiza Gonzalez-Garcia:** Supervision, Writing – review & editing. **Arjan Mol:** Conceptualization, Supervision, Writing – review & editing.

Declaration of competing interest

The authors declare no competing interests.

Acknowledgements

The authors wish to acknowledge the financial support from the China Scholarship Council (CSC) and the collaboration agreement between AkzoNobel and Delft University of Technology.

References

[1] N.L. Sukiman, X. Zhou, N. Birbilis, A.E. Hughes, J.M.C. Mol, S. J, X. Zhou, G. E, Durability and corrosion of aluminium and its alloys: overview, property space, techniques and developments, in: Z. Ahmad (Ed.), Aluminium Alloys-New Trends in Fabrication and Applications, InTech, 2012, https://doi.org/10.5772/53752.

[2] A.E. Hughes, C. MacRae, N. Wilson, A. Torpy, T.H. Muster, A.M. Glenn, Sheet AA2024-T3: a new investigation of microstructure and composition, Surface and Interface Analysis 42 (2010) 334–338, https://doi.org/10.1002/sia.3163.

[3] A. Boag, A.E. Hughes, N.C. Wilson, A. Torpy, C.M. MacRae, A.M. Glenn, T. H. Muster, How complex is the microstructure of AA2024-T3? Corros. Sci. 51 (2009) 1565–1568, https://doi.org/10.1016/j.corsci.2009.05.001.

[4] A. E., N. Birbilis, J. M.C., S. J., X. Zhou, G. E, High strength Al-alloys: microstructure, corrosion and principles of protection, in: Z. Ahmad (Ed.), Recent Trends in Processing and Degradation of Aluminium Alloys, InTech, 2011, https://doi.org/10.5772/18766.

[5] J.L. García-Hernández, C.G. Garay-Reyes, I.K. Gómez-Barraza, M.A. Ruiz-Esparza-Rodríguez, E.J. Gutiérrez-Castañeda, I. Estrada-Guel, M.C. Maldonado-Orozco, R. Martínez-Sánchez, Influence of plastic deformation and Cu/Mg ratio on the strengthening mechanisms and precipitation behavior of AA2024 aluminum alloys, J. Mater. Res. Technol. 8 (2019) 5471–5475, https://doi.org/10.1016/j.jmrt.2019.09.015.

[6] S.J. Andersen, C.D. Marioara, J. Friis, S. Wenner, R. Holmestad, Precipitates in aluminium alloys, Advances in Physics: X. 3 (2018) 1479984, https://doi.org/10.1080/23746149.2018.1479984.

[7] C. Blanc, B. Lavelle, G. Mankowski, The role of precipitates enriched with copper on the susceptibility to pitting corrosion of the 2024 aluminium alloy, Corros. Sci. 39 (1997) 495–510, https://doi.org/10.1016/S0010-938X(97)86099-4.

[8] N. Birbilis, Y.M. Zhu, S.K. Kairy, M.A. Glenn, J.-F. Nie, A.J. Morton, Y. Gonzalez-Garcia, H. Terryn, J.M.C. Mol, A.E. Hughes, A closer look at constituent induced localised corrosion in Al-Cu-Mg alloys, Corros. Sci. 113 (2016) 160–171, https://doi.org/10.1016/j.corsci.2016.10.018.

[9] A.E. Hughes, J.M.C. Mol, M.L. Zheludkevich, R.G. Buchheit (Eds.), Active Protective Coatings: New-Generation Coatings for Metals, Springer, Netherlands, Dordrecht, 2016, https://doi.org/10.1007/978-94-017-7540-3.

[10] G.O. Ilevbare, J.R. Scully, J. Yuan, R.G. Kelly, Inhibition of pitting corrosion on aluminum alloy 2024-T3: effect of soluble chromate additions vs chromate conversion coating, Corrosion 56 (2000).

[11] A.E. Hughes, R.J. Taylor, B.R.W. Hinton, Chromate conversion coatings on 2024 Al alloy, Surface and Interface Analysis 25 (1997) 223–234, https://doi.org/10.1002/(SICI)1096-9918(199704)25:4<223::AID-SIA225>3.0.CO;2-D.

[12] P. Campestrini, H. Terryn, J. Vereecken, J.H.W. de Wit, Chromate conversion coating on aluminum alloys: III. Corrosion protection, J. Electrochem. Soc. 151 (2004) B370, https://doi.org/10.1149/1.1736683.

[13] O. Gharbi, S. Thomas, C. Smith, N. Birbilis, Chromate replacement: what does the future hold? Npj Mater Degrad. 2 (2018) 12, https://doi.org/10.1038/s41529-018-0034-5.

[14] T. Prosek, D. Thierry, A model for the release of chromate from organic coatings, Prog. Org. Coat. 49 (2004) 209–217, https://doi.org/10.1016/j.porgcoat.2003.09.012.

[15] M. Kendig, S. Jeanjaquet, R. Addison, J. Waldrop, Role of hexavalent chromium in the inhibition of corrosion of aluminum alloys, Surf. Coat. Technol. 140 (2001) 58–66, https://doi.org/10.1016/S0257-8972(01)01099-4.

[16] R. Saha, R. Nandi, B. Saha, Sources and toxicity of hexavalent chromium, J. Coord. Chem. 64 (2011) 1782–1806, https://doi.org/10.1080/00958972.2011.583646.
[17] P. Visser, H. Terryn, J.M.C. Mol, Aerospace Coatings, in: A.E. Hughes, J.M.C. Mol, M.L. Zheludkevich, R.G. Buchheit (Eds.), Active Protective Coatings: New-Generation Coatings for Metals, Springer, Netherlands, Dordrecht, 2016, pp. 315–372, https://doi.org/10.1007/978-94-017-7540-3_12.
[18] M. Becker, Chromate-free chemical conversion coatings for aluminum alloys, Corrosion Rev. 37 (2019) 321–342, https://doi.org/10.1515/corrrev-2019-0032.
[19] I. Milošev, G.S. Frankel, Review—conversion coatings based on zirconium and/or titanium, J. Electrochem. Soc. 165 (2018) C127, https://doi.org/10.1149/2.0371803jes.
[20] R.G. Buchheit, M.D. Bode, G.E. Stoner, Corrosion-resistant, chromate-free talc coatings for aluminum, Corrosion 50 (1994) 205–214, https://doi.org/10.5006/1.3293512.
[21] M.W. Kendig, R.G. Buchheit, Corrosion inhibition of aluminum and aluminum alloys by soluble chromates, chromate coatings, and chromate-free coatings, Corrosion 59 (2003) 379–400, https://doi.org/10.5006/1.3277570.
[22] R. Berger, U. Bexell, T. Mikael Grehk, S.-E. Hörnström, A comparative study of the corrosion protective properties of chromium and chromium free passivation methods, Surf. Coat. Technol. 202 (2007) 391–397, https://doi.org/10.1016/j.surfcoat.2007.06.001.
[23] L. Selegård, T. Poot, P. Eriksson, J. Palisaitis, P.O.Å. Persson, Z. Hu, K. Uvdal, In-situ growth of cerium nanoparticles for chrome-free, corrosion resistant anodic coatings, Surf. Coat. Technol. 410 (2021) 126958, https://doi.org/10.1016/j.surfcoat.2021.126958.
[24] Y. Castro, E. Özmen, A. Durán, Integrated self-healing coating system for outstanding corrosion protection of AA2024, Surf. Coat. Technol. 387 (2020) 125521, https://doi.org/10.1016/j.surfcoat.2020.125521.
[25] O. Lopez-Garrity, G.S. Frankel, Corrosion inhibition of aluminum alloy 2024-T3 by sodium molybdate, J. Electrochem. Soc. 161 (2013) C95, https://doi.org/10.1149/2.044403jes.
[26] D.S. Kharitonov, J. Sommertune, C. Örnek, J. Ryl, I.I. Kurilo, P.M. Claesson, J. Pan, Corrosion inhibition of aluminium alloy AA6063-T5 by vanadates: local surface chemical events elucidated by confocal Raman micro-spectroscopy, Corros. Sci. 148 (2019) 237–250, https://doi.org/10.1016/j.corsci.2018.12.011.
[27] V. Moutarlier, M.P. Gigandet, B. Normand, J. Pagetti, EIS characterisation of anodic films formed on 2024 aluminium alloy, in sulphuric acid containing molybdate or permanganate species, Corros. Sci. 47 (2005) 937–951, https://doi.org/10.1016/j.corsci.2004.06.019.
[28] J.-A. Hill, T. Markley, M. Forsyth, P.C. Howlett, B.R.W. Hinton, Corrosion inhibition of 7000 series aluminium alloys with cerium diphenyl phosphate, J. Alloys Compd. 509 (2011) 1683–1690, https://doi.org/10.1016/j.jallcom.2010.09.151.
[29] D.O. Flamini, M. Trueba, S.P. Trasatti, Aniline-based silane as a primer for corrosion inhibition of aluminium, Prog. Org. Coat. 74 (2012) 302–310, https://doi.org/10.1016/j.porgcoat.2011.11.011.
[30] V. Dalmoro, J.H.Z. dos Santos, E. Armelin, C. Alemán, D.S. Azambuja, Sol–gel hybrid films based on organosilane and montmorillonite for corrosion inhibition of AA2024, J. Colloid Interface Sci. 426 (2014) 308–313, https://doi.org/10.1016/j.jcis.2014.04.021.
[31] A.K. Mishra, R. Balasubramaniam, Corrosion inhibition of aluminum alloy AA 2014 by rare earth chlorides, Corros. Sci. 49 (2007) 1027–1044, https://doi.org/10.1016/j.corsci.2006.06.026.
[32] K.A. Yasakau, M.L. Zheludkevich, S.V. Lamaka, M.G.S. Ferreira, Mechanism of corrosion inhibition of AA2024 by rare-earth compounds, J. Phys. Chem. B 110 (2006) 5515–5528, https://doi.org/10.1021/jp0560664.
[33] M.B. Jensen, M.J. Peterson, N. Jadhav, V.J. Gelling, SECM investigation of corrosion inhibition by tungstate- and vanadate-doped polypyrrole/aluminum flake composite coatings on AA2024-T3, Prog. Org. Coat. 77 (2014) 2116–2122, https://doi.org/10.1016/j.porgcoat.2014.05.019.
[34] R. Samiee, B. Ramezanzadeh, M. Mahdavian, E. Alibakhshi, Corrosion inhibition performance and healing ability of a hybrid silane coating in the presence of praseodymium (III) cations, J. Electrochem. Soc. 165 (2018) C777, https://doi.org/10.1149/2.0841811jes.
[35] J. Lin, D. Battocchi, G.P. Bierwagen, Inhibitors for prolonging corrosion protection of Mg-rich primer on Al alloy 2024-T3, J Coat Technol Res. 14 (2017) 497–504, https://doi.org/10.1007/s11998-016-9875-4.
[36] X. Wang, G.S. Frankel, Protection mechanism of Al-rich epoxy primer on aluminum alloy 2024-T3, Corrosion 73 (2017) 1192–1195, https://doi.org/10.5006/2526.
[37] C.A. Drewien, M.O. Eatough, D.R. Tallant, C.R. Hills, R.G. Buchheit, Lithium-aluminum-carbonate-hydroxide hydrate coatings on aluminum alloys: composition, structure, and processing bath chemistry, J. Mater. Res. 11 (1996) 1507–1513, https://doi.org/10.1557/JMR.1996.0188.
[38] J. Gui, T.M. Devine, Influence of lithium on the corrosion of aluminum, Scr. Metall.; (United States) 21 (6) (1987), https://doi.org/10.1016/0036-9748(87)90336-X.
[39] P. Visser, Y. Liu, X. Zhou, T. Hashimoto, G.E. Thompson, S.B. Lyon, L.G.J. van der Ven, A.J.M.C. Mol, H.A. Terryn, The corrosion protection of AA2024-T3 aluminium alloy by leaching of lithium-containing salts from organic coatings, Faraday Discuss. 180 (2015) 511–526, https://doi.org/10.1039/C4FD00237G.
[40] Y. Liu, P. Visser, X. Zhou, S.B. Lyon, T. Hashimoto, M. Curioni, A. Gholinia, G. E. Thompson, G. Smyth, S.R. Gibbon, D. Graham, J.M.C. Mol, H. Terryn, Protective film formation on AA2024-T3 aluminum alloy by leaching of lithium carbonate from an organic coating, J. Electrochem. Soc. 163 (2015) C45, https://doi.org/10.1149/2.0021603jes.
[41] Y. Liu, P. Visser, X. Zhou, S.B. Lyon, T. Hashimoto, A. Gholinia, G.E. Thompson, G. Smyth, S.R. Gibbon, D. Graham, J.M.C. Mol, H. Terryn, An investigation of the corrosion inhibitive layers generated from lithium oxalate-containing organic coating on AA2024-T3 aluminium alloy, Surface and Interface Analysis 48 (2016) 798–803, https://doi.org/10.1002/sia.5972.
[42] P. Visser, Y. Liu, H. Terryn, J.M.C. Mol, Lithium salts as leachable corrosion inhibitors and potential replacement for hexavalent chromium in organic coatings for the protection of aluminum alloys, J. Coat. Technol. Res. 13 (2016) 557–566, https://doi.org/10.1007/s11998-016-9784-6.
[43] P. Visser, A. Lutz, J.M.C. Mol, H. Terryn, Study of the formation of a protective layer in a defect from lithium-leaching organic coatings, Prog. Org. Coat. 99 (2016) 80–90, https://doi.org/10.1016/j.porgcoat.2016.04.028.
[44] R.G. Buchheit, F.D. Wall, G.E. Stoner, J.P. Moran, Anodic dissolution-based mechanism for the rapid cracking, preexposure phenomenon demonstrated by aluminum-lithium-copper alloys, Corrosion 51 (1995).
[45] C.M. Rangel, M.A. Travassos, The passivation of aluminium in lithium carbonate/bicarbonate solutions, Corros. Sci. 33 (1992) 327–343, https://doi.org/10.1016/0010-938X(92)90064-A.
[46] C.M. Rangel, M.A. Travassos, Li-based conversion coatings on aluminium: an electrochemical study of coating formation and growth, Surf. Coat. Technol. 200 (2006) 5823–5828, https://doi.org/10.1016/j.surfcoat.2005.08.145.
[47] R.G. Buchheit, G.E. Stoner, Chromate-Free Corrosion Resistant Talc Coatings for Aluminum Alloys, Sandia National Labs, Albuquerque, NM (United States), 1992. https://www.osti.gov/biblio/6725477.
[48] R.G. Buchheit, C.A. Drewien, M.A. Martinez, G.E. Stoner, Chromate-Free Corrosion Resistant Conversion Coatings for Aluminum Alloys, Sandia National Lab. (SNL-NM), Albuquerque, NM (United States), 1995, https://doi.org/10.2172/28379.
[49] C.A. Drewien, R.G. Buchheit, Issues for Conversion Coating of Aluminum Alloys with Hydrotalcite, Sandia National Labs, Albuquerque, NM (United States), 1993. https://www.osti.gov/biblio/10107499.
[50] R.G. Buchheit, Alkaline Oxide Conversion Coatings for Aluminum Alloys, Sandia National Lab. (SNL-NM), Albuquerque, NM (United States), 1996. https://www.osti.gov/biblio/195749.
[51] R.G. Buchheit, M.A. Martinez, C.B. Cooper, Corrosion resistant coatings for aluminum by hydrothermal film formation in alkaline Li-salt solutions, MRS Online Proceedings Library (OPL). 432 (1996) 273, https://doi.org/10.1557/PROC-432-273.
[52] R.G. Buchheit, Copper removal during formation of corrosion resistant alkaline oxide coatings on Al–Cu–Mg alloys, J. Appl. Electrochem. 28 (1998) 503–510, https://doi.org/10.1023/A:1003217211727.
[53] R.B. Leggat, W. Zhang, R.G. Buchheit, S.R. Taylor, Performance of hydrotalcite conversion treatments on AA2024-T3 when used in a coating system, Corrosion 58 (2002) 322–328, https://doi.org/10.5006/1.3287681.
[54] W. Zhang, R.G. Buchheit, Hydrotalcite coating formation on Al-Cu-Mg alloys from oxidizing bath chemistries, Corrosion 58 (2002) 591–600, https://doi.org/10.5006/1.3277650.
[55] F. Wong, R.G. Buchheit, Utilizing the structural memory effect of layered double hydroxides for sensing water uptake in organic coatings, Prog. Org. Coat. 51 (2004) 91–102, https://doi.org/10.1016/j.porgcoat.2004.07.001.
[56] O. Lunder, J.C. Walmsley, P. Mack, K. Nisancioglu, Formation and characterisation of a chromate conversion coating on AA6060 aluminium, Corros. Sci. 47 (2005) 1604–1624, https://doi.org/10.1016/j.corsci.2004.08.012.
[57] G.R. Williams, D. O'Hare, A kinetic study of the intercalation of lithium salts into Al(OH)3, J. Phys. Chem. B 110 (2006) 10619–10629, https://doi.org/10.1021/jp057130k.
[58] C.J. Wang, D. O'Hare, Topotactic synthesis of layered double hydroxide nanorods, J. Mater. Chem. 22 (2012) 23064–23070, https://doi.org/10.1039/C2JM34670B.
[59] B. Pillado, B. Mingo, R. del Olmo, E. Matykina, A.M. Kooijman, Y. Gonzalez-Garcia, R. Arrabal, M. Mohedano, LDH conversion films for active protection of AZ31 Mg alloy, Journal of Magnesium and Alloys. 11 (2023) 201–216, https://doi.org/10.1016/j.jma.2022.09.014.
[60] D. Mata, M. Serdechnova, M. Mohedano, C.L. Mendis, S.V. Lamaka, J. Tedim, T. Hack, S. Nixon, M.L. Zheludkevich, Hierarchically organized Li–Al-LDH nano-flakes: a low-temperature approach to seal porous anodic oxide on aluminum alloys, RSC Adv. 7 (2017) 35357–35367, https://doi.org/10.1039/C7RA05593E.
[61] R.G. Buchheit, S.B. Mamidipally, P. Schmutz, H. Guan, Active corrosion protection in Ce-modified hydrotalcite conversion coatings, Corrosion 58 (2002) 3–14, https://doi.org/10.5006/1.3277303.
[62] P. Visser, Y. Gonzalez-Garcia, J.M.C. Mol, H. Terryn, Mechanism of passive layer formation on AA2024-T3 from alkaline lithium carbonate solutions in the presence of sodium chloride, J. Electrochem. Soc. 165 (2018) C60–C70, https://doi.org/10.1149/2.1011802jes.
[63] Z. Li, A. Homborg, Y. Gonzalez-Garcia, A. Kosari, P. Visser, A. Mol, Evaluation of the formation and protectiveness of a lithium-based conversion layer using electrochemical noise, Electrochim. Acta 426 (2022) 140733, https://doi.org/10.1016/j.electacta.2022.140733.
[64] Z. Li, A. Homborg, Y. Gonzalez-Garcia, P. Visser, M. Soleimani, A. Mol, The effect of ambient ageing on the corrosion protective properties of a lithium-based conversion layer, J. Electrochem. Soc. 170 (2023) 031504, https://doi.org/10.1149/1945-7111/acc1a6.
[65] Z. Li, G. Li, P. Visser, A. Homborg, Y. Gonzalez-Garcia, A. Mol, Local scanning electrochemical microscopy analysis of a lithium-based conversion layer on

AA2024-T3 at progressive stages of formation, Electrochim. Acta 469 (2023) 143270, https://doi.org/10.1016/j.electacta.2023.143270.
[66] P. Visser, K. Marcoen, G.F. Trindade, M.-L. Abel, J.F. Watts, T. Hauffman, J.M. C. Mol, H. Terryn, The chemical throwing power of lithium-based inhibitors from organic coatings on AA2024-T3, Corros. Sci. 150 (2019) 194–206, https://doi.org/10.1016/j.corsci.2019.02.009.
[67] K. Marcoen, P. Visser, G.F. Trindade, M.-L. Abel, J.F. Watts, J.M.C. Mol, H. Terryn, T. Hauffman, Compositional study of a corrosion protective layer formed by leachable lithium salts in a coating defect on AA2024-T3 aluminium alloys, Prog. Org. Coat. 119 (2018) 65–75, https://doi.org/10.1016/j.porgcoat.2018.02.011.
[68] A. Trentin, S.V. Harb, M.C. Uvida, S.H. Pulcinelli, C.V. Santilli, K. Marcoen, S. Pletincx, H. Terryn, T. Hauffman, P. Hammer, Dual role of lithium on the structure and self-healing ability of PMMA-silica coatings on AA7075 alloy, ACS Appl. Mater. Interfaces 11 (2019) 40629–40641, https://doi.org/10.1021/acsami.9b13839.
[69] J.S. Laird, P. Visser, S. Ranade, A.E. Hughes, H. Terryn, J.M.C. Mol, Li leaching from lithium carbonate-primer: an emerging perspective of transport pathway development, Prog. Org. Coat. 134 (2019) 103–118, https://doi.org/10.1016/j.porgcoat.2019.04.062.
[70] P. Visser, S. Ranade, J.S. Laird, A.M. Glenn, A.E. Hughes, H. Terryn, J.M.C. Mol, Li leaching from Li carbonate-primer: transport pathway development from the scribe edge of a primer/topcoat system, Prog. Org. Coat. 158 (2021) 106284, https://doi.org/10.1016/j.porgcoat.2021.106284.
[71] X. Li, S. Caes, T. Pardoen, G. De Schutter, T. Hauffman, B. Kursten, Inhibition effect of lithium salts on the corrosion of AA1100 aluminium alloy in ordinary Portland cement pastes, Corros. Sci. 221 (2023) 111325, https://doi.org/10.1016/j.corsci.2023.111325.
[72] A. Kosari, F. Tichelaar, P. Visser, P. Taheri, H. Zandbergen, H. Terryn, J.M.C. Mol, Nanoscopic and in-situ cross-sectional observations of Li-based conversion coating formation using liquid-phase TEM, Npj Mater Degrad. 5 (2021) 40, https://doi.org/10.1038/s41529-021-00189-y.
[73] C. Jing, B. Dong, A. Raza, T. Zhang, Y. Zhang, Corrosion inhibition of layered double hydroxides for metal-based systems, Nano, Mater. Sci. 3 (2021) 47–67, https://doi.org/10.1016/j.nanoms.2020.12.001.
[74] D. Tonelli, I. Gualandi, E. Musella, E. Scavetta, Synthesis and characterization of layered double hydroxides as materials for electrocatalytic applications, Nanomaterials 11 (2021) 725, https://doi.org/10.3390/nano11030725.
[75] M.A. Iqbal, L. Sun, A.T. Barrett, M. Fedel, Layered double hydroxide protective films developed on aluminum and aluminum alloys: synthetic methods and anti-corrosion mechanisms, Coatings 10 (2020) 428, https://doi.org/10.3390/coatings10040428.
[76] Y. Cao, D. Zheng, F. Zhang, J. Pan, C. Lin, Layered double hydroxide (LDH) for multi-functionalized corrosion protection of metals: a review, Journal of Materials Science & Technology. 102 (2022) 232–263, https://doi.org/10.1016/j.jmst.2021.05.078.
[77] A.C. Bouali, M. Serdechnova, C. Blawert, J. Tedim, M.G.S. Ferreira, M. L. Zheludkevich, Layered double hydroxides (LDHs) as functional materials for the corrosion protection of aluminum alloys: a review, Appl. Mater. Today 21 (2020) 100857, https://doi.org/10.1016/j.apmt.2020.100857.
[78] A.C. Bouali, M.H. Iuzviuk, M. Serdechnova, K.A. Yasakau, D. Drozdenko, A. Lutz, K. Fekete, G. Dovzhenko, D.C.F. Wieland, H. Terryn, M.G.S. Ferreira, I. A. Zobkalo, M.L. Zheludkevich, Mechanism of LDH direct growth on aluminum alloy surface: a kinetic and morphological approach, J. Phys. Chem. C 125 (2021) 11687–11701, https://doi.org/10.1021/acs.jpcc.1c02281.
[79] I. Mohammadi, T. Shahrabi, M. Mahdavian, M. Izadi, Zn-Al layered double hydroxide as an inhibitive conversion coating developed on AA2024-T3 by one-step hydrothermal crystallization: crystal structure evolution and corrosion protection performance, Surf. Coat. Technol. 409 (2021) 126882, https://doi.org/10.1016/j.surfcoat.2021.126882.
[80] K. Lin, X. Luo, X. Pan, C. Zhang, Y. Liu, Enhanced corrosion resistance of LiAl-layered double hydroxide (LDH) coating modified with a Schiff base salt on aluminum alloy by one step in-situ synthesis at low temperature, Appl. Surf. Sci. 463 (2019) 1085–1096, https://doi.org/10.1016/j.apsusc.2018.09.034.
[81] A.C. Bouali, M.H. Iuzviuk, M. Serdechnova, K.A. Yasakau, D.C.F. Wieland, G. Dovzhenko, H. Maltanava, I.A. Zobkalo, M.G.S. Ferreira, M.L. Zheludkevich, Zn-Al LDH growth on AA2024 and zinc and their intercalation with chloride: comparison of crystal structure and kinetics, Appl. Surf. Sci. 501 (2020) 144027, https://doi.org/10.1016/j.apsusc.2019.144027.
[82] I. Mohammadi, T. Shahrabi, M. Mahdavian, M. Izadi, Chemical modification of LDH conversion coating with diethyldithiocarbamate as a novel anti-corrosive film for AA2024-T3, J. Ind. Eng. Chem. 95 (2021) 134–147, https://doi.org/10.1016/j.jiec.2020.12.016.
[83] D.E.L. Vieira, A.N. Salak, M.G.S. Ferreira, J.M. Vieira, C.M.A. Brett, Ce-substituted Mg-Al layered double hydroxides to prolong the corrosion protection lifetime of aluminium alloys, Appl. Surf. Sci. 573 (2022) 151527, https://doi.org/10.1016/j.apsusc.2021.151527.
[84] D. Álvarez, A. Collazo, M. Hernández, X.R. Nóvoa, C. Pérez, Characterization of hybrid sol–gel coatings doped with hydrotalcite-like compounds to improve corrosion resistance of AA2024-T3 alloys, Prog. Org. Coat. 68 (2010) 91–99, https://doi.org/10.1016/j.porgcoat.2009.09.023.
[85] A. Collazo, M. Hernández, X.R. Nóvoa, C. Pérez, Effect of the addition of thermally activated hydrotalcite on the protective features of sol–gel coatings applied on AA2024 aluminium alloys, Electrochim. Acta 56 (2011) 7805–7814, https://doi.org/10.1016/j.electacta.2011.03.067.
[86] E. Alibakhshi, E. Ghasemi, M. Mahdavian, B. Ramezanzadeh, A comparative study on corrosion inhibitive effect of nitrate and phosphate intercalated Zn-Al-layered double hydroxides (LDHs) nanocontainers incorporated into a hybrid silane layer and their effect on cathodic delamination of epoxy topcoat, Corros. Sci. 115 (2017) 159–174, https://doi.org/10.1016/j.corsci.2016.12.001.
[87] A.M. Fogg, D. O'Hare, Study of the intercalation of lithium salt in gibbsite using time-resolved in situ X-ray diffraction, Chem. Mater. 11 (1999) 1771–1775, https://doi.org/10.1021/cm981151s.
[88] K.A. Tarasov, V.P. Isupov, L.E. Chupakhina, D. O'Hare, A time resolved, in-situ X-ray diffraction study of the de-intercalation of anions and lithium cations from [LiAl2(OH)6]nX·qH2O (X = Cl−, Br−, NO3−, SO42−), J. Mater. Chem. 14 (2004) 1443–1447, https://doi.org/10.1039/B314473A.
[89] L. Huang, J. Wang, Y. Gao, Y. Qiao, Q. Zheng, Z. Guo, Y. Zhao, D. O'Hare, Q. Wang, Synthesis of LiAl2-layered double hydroxides for CO2 capture over a wide temperature range, J. Mater. Chem. A 2 (2014) 18454–18462, https://doi.org/10.1039/C4TA04065A.
[90] J. Chen, H. Yuan, J. Yu, M. Yan, Y. Yang, S. Lin, Regulating lithium extraction based on intercalated SO42− in Li/Al-LDHs, J. Colloid Interface Sci. 649 (2023) 694–702, https://doi.org/10.1016/j.jcis.2023.06.165.
[91] Y. Lee, D.-Y. Jung, Lithium intercalation and deintercalation of thermally decomposed LiAl2-layered double hydroxides, Appl. Clay Sci. 228 (2022) 106631, https://doi.org/10.1016/j.clay.2022.106631.
[92] Y. Lee, J.-H. Cha, D.-Y. Jung, Lithium separation by growth of lithium aluminum layered double hydroxides on aluminum metal substrates, Solid State Sci. 110 (2020) 106488, https://doi.org/10.1016/j.solidstatesciences.2020.106488.
[93] S.-L. Wang, C.-H. Lin, Y.-Y. Yan, M.K. Wang, Synthesis of Li/Al LDH using aluminum and LiOH, Applied Clay Science. 72 (2013) 191–195, https://doi.org/10.1016/j.clay.2013.02.001.
[94] V. Kasneryk, M. Serdechnova, C. Blawert, M.L. Zheludkevich, LDH has been grown: what is next? Overview on methods of post-treatment of LDH conversion coatings, Applied Clay Science 232 (2023) 106774, https://doi.org/10.1016/j.clay.2022.106774.
[95] H.N. McMurray, G. Williams, Inhibition of filiform corrosion on organic-coated aluminum alloy by hydrotalcite-like anion-exchange pigments, Corrosion 60 (2004) 219–228, https://doi.org/10.5006/1.3287724.
[96] Y. Su, S. Qiu, D. Yang, S. Liu, H. Zhao, L. Wang, Q. Xue, Active anti-corrosion of epoxy coating by nitrite ions intercalated MgAl LDH, J. Hazard. Mater. 391 (2020) 122215, https://doi.org/10.1016/j.jhazmat.2020.122215.
[97] T. Yan, S. Xu, Q. Peng, L. Zhao, X. Zhao, X. Lei, F. Zhang, Self-healing of layered double hydroxide film by dissolution/recrystallization for corrosion protection of aluminum, J. Electrochem. Soc. 160 (2013) C480, https://doi.org/10.1149/2.053310jes.
[98] B. Yang, Y. Ma, Z. Liang, Y. Liao, Z. Wang, P. Zhu, A superhydrophobic and corrosion resistant layered double hydroxides coating on AA2099-T83 Al-Cu-Li alloy, Surf. Coat. Technol. 405 (2021) 126629, https://doi.org/10.1016/j.surfcoat.2020.126629.
[99] J. Li, K. Lin, X. Luo, H. Zhang, Y.F. Cheng, X. Li, Y. Liu, Enhanced corrosion protection property of Li-Al layered double hydroxides (LDHs) film modified by 2-guanidinosuccinic acid with excellent self-repairing and self-antibacterial properties, Appl. Surf. Sci. 480 (2019) 384–394, https://doi.org/10.1016/j.apsusc.2019.02.164.
[100] T. Hurlen, A.T. Haug, Corrosion and passive behaviour of aluminium in weakly alkaline solution, Electrochim. Acta 29 (1984) 1133–1138, https://doi.org/10.1016/0013-4686(84)87167-4.
[101] A. Kosari, F. Tichelaar, P. Visser, H. Zandbergen, H. Terryn, J.M.C. Mol, Laterally-resolved formation mechanism of a lithium-based conversion layer at the matrix and intermetallic particles in aerospace aluminium alloys, Corros. Sci. 190 (2021) 109651, https://doi.org/10.1016/j.corsci.2021.109651.
[102] V.P. Isupov, Intercalation compounds of aluminum hydroxide, J. Struct. Chem. 40 (1999) 672–685, https://doi.org/10.1007/BF02903444.
[103] T.P. Belova, Experimental studies in the sorptive extraction of boron and lithium from thermal waters, J. Volcanolog. Seismol. 11 (2017) 136–142, https://doi.org/10.1134/S0742046317020026.
[104] M. Yu, H. Li, N. Du, W. Hou, Understanding Li-Al-CO3 layered double hydroxides. (I) Urea-supported hydrothermal synthesis, J. Colloid Interface Sci. 547 (2019) 183–189, https://doi.org/10.1016/j.jcis.2019.03.101.
[105] A. Kosari, P. Visser, F. Tichelaar, S. Eswara, J.-N. Audinot, T. Wirtz, H. Zandbergen, H. Terryn, J.M.C. Mol, Cross-sectional characterization of the conversion layer formed on AA2024-T3 by a lithium-leaching coating, Appl. Surf. Sci. 512 (2020) 145665, https://doi.org/10.1016/j.apsusc.2020.145665.
[106] P. Visser, M. Meeusen, Y. Gonzalez-Garcia, H. Terryn, J.M.C. Mol, Electrochemical evaluation of corrosion inhibiting layers formed in a defect from lithium-leaching organic coatings, J. Electrochem. Soc. 164 (2017) C396–C406, https://doi.org/10.1149/2.1411707jes.
[107] P. Visser, S.A. Hayes, Low-temperature-curable coating composition useful as anticorrosive primer coating for non-ferrous metal substrates, particularly aluminum or aluminum alloy, comprises film-forming resin, curing agent, and lithium salt, patent nr, WO2010112605-A1 (2010). WO2010112605A1, 2010.
[108] P. Visser, H. Terryn, J.M.C. Mol, On the importance of irreversibility of corrosion inhibitors for active coating protection of AA2024-T3, Corros. Sci. 140 (2018) 272–285, https://doi.org/10.1016/j.corsci.2018.05.037.
[109] I. Recloux, F. Andreatta, M.-E. Druart, L.B. Coelho, C. Cepek, D. Cossement, L. Fedrizzi, M.-G. Olivier, Stability of benzotriazole-based films against AA2024 aluminium alloy corrosion process in neutral chloride electrolyte, J. Alloys Compd. 735 (2018) 2512–2522, https://doi.org/10.1016/j.jallcom.2017.11.346.

[110] A.C. Balaskas, M. Curioni, G.E. Thompson, Effectiveness of 2-mercaptobenzothiazole, 8-hydroxyquinoline and benzotriazole as corrosion inhibitors on AA 2024-T3 assessed by electrochemical methods, Surface and Interface Analysis 47 (2015) 1029–1039, https://doi.org/10.1002/sia.5810.
[111] P. Visser, H. Terryn, J.M.C. Mol, Active corrosion protection of various aluminium alloys by lithium-leaching coatings, Surface and Interface Analysis 51 (2019) 1276–1287, https://doi.org/10.1002/sia.6638.
[112] M. Meeusen, P. Visser, L. Fernández Macía, A. Hubin, H. Terryn, J.M.C. Mol, The use of odd random phase electrochemical impedance spectroscopy to study lithium-based corrosion inhibition by active protective coatings, Electrochim. Acta 278 (2018) 363–373, https://doi.org/10.1016/j.electacta.2018.05.036.
[113] J. Li, B. Hurley, R. Buchheit, Microelectrochemical characterization of the effect of rare earth inhibitors on the localized corrosion of AA2024-T3, J. Electrochem. Soc. 162 (2015) C563, https://doi.org/10.1149/2.0791510jes.
[114] T. Suter, H. Böhni, A new microelectrochemical method to study pit initiation on stainless steels, Electrochim. Acta 42 (1997) 3275–3280, https://doi.org/10.1016/S0013-4686(70)01783-8.
[115] J.R. Scully, F. Presuel-Moreno, M. Goldman, R.G. Kelly, N. Tailleart, User-selectable barrier, sacrificial anode, and active corrosion inhibiting properties of Al-Co-Ce alloys for coating applications, Corrosion 64 (2008) 210–229, https://doi.org/10.5006/1.3278467.
[116] B. Kannan, C.F. Glover, H.N. McMurray, G. Williams, J.R. Scully, Performance of a magnesium-rich primer on pretreated AA2024-T351 in full immersion: a galvanic throwing power investigation using a scanning vibrating electrode technique, J. Electrochem. Soc. 165 (2018) C27, https://doi.org/10.1149/2.0711802jes.
[117] J.R. Scully, N. Tailleart, F. Presuel-Moreno, 9- Tunable multifunctional corrosion-resistant metallic coatings containing rare earth elements, in: M. Forsyth, B. Hinton (Eds.), Rare Earth-Based Corrosion Inhibitors, Woodhead Publishing, 2014, pp. 267–290, https://doi.org/10.1533/9780857093585.267.
[118] A. Hughes, J. Laird, C. Ryan, P. Visser, H. Terryn, A. Mol, Particle characterisation and depletion of Li2CO3 inhibitor in a polyurethane coating, Coatings 7 (2017) 106, https://doi.org/10.3390/coatings7070106.
[119] R.T. Foley, Localized corrosion of aluminum alloys—a review, Corrosion 42 (1986) 277–288, https://doi.org/10.5006/1.3584905.
[120] R.T. Foley, T.H. Nguyen, The chemical nature of aluminum corrosion: V. Energy transfer in aluminum dissolution, J. Electrochem. Soc. 129 (1982) 464, https://doi.org/10.1149/1.2123881.
[121] L. Anicăi, A.C. Manea, T. Visan, Lithium-aluminium hydroxide hydrate thin layers on Al based substrates-new ecological process for corrosion resistance increase, Mol. Cryst. Liq. Cryst. 418 (2004) 41–53, https://doi.org/10.1080/15421400490478948.
[122] M.R. Tabrizi, S.B. Lyon, G.E. Thompson, J.M. Ferguson, The long-term corrosion of aluminium in alkaline media, Corros. Sci. 32 (1991) 733–742, https://doi.org/10.1016/0010-938X(91)90087-6.
[123] A.E. Hughes, A. Trinchi, F.F. Chen, Y.S. Yang, I.S. Cole, S. Sellaiyan, J. Carr, P. D. Lee, G.E. Thompson, T.Q. Xiao, Revelation of intertwining organic and inorganic fractal structures in polymer coatings, Adv. Mater. 26 (2014) 4504–4508, https://doi.org/10.1002/adma.201400561.
[124] A.E. Hughes, A. Trinchi, F.F. Chen, Y.S. Yang, S. Sellaiyan, J. Carr, P.D. Lee, G. E. Thompson, T.Q. Xiao, Structure and transport in coatings from multiscale computed tomography of coatings—new perspectives for eelectrochemical impedance spectroscopy modeling? Electrochim. Acta 202 (2016) 243–252, https://doi.org/10.1016/j.electacta.2015.10.183.
[125] S. Sellaiyan, A.E. Hughes, S.V. Smith, A. Uedono, J. Sullivan, S. Buckman, Leaching properties of chromate-containing epoxy films using radiotracers, PALS and SEM, Prog. Org. Coat. 77 (2014) 257–267, https://doi.org/10.1016/j.porgcoat.2013.09.014.
[126] J.S. Laird, A.E. Hughes, C.G. Ryan, P. Visser, H. Terryn, J.M.C. Mol, Particle induced gamma and X-ray emission spectroscopies of lithium based alloy coatings, Nucl. Instrum. Methods Phys. Res., Sect. B 404 (2017) 167–172, https://doi.org/10.1016/j.nimb.2017.03.088.
[127] S.Gh.R. Emad, X. Zhou, S.B. Lyon, G.E. Thompson, Y. Liu, G. Smyth, D. Graham, D. Francis, S.R. Gibbon, Influence of volume concentration of active inhibitor on microstructure and leaching behaviour of a model primer, Prog. Org. Coat. 102 (2017) 71–81, https://doi.org/10.1016/j.porgcoat.2016.04.039.
[128] E. Javierre, S.J. García, J.M.C. Mol, F.J. Vermolen, C. Vuik, S. van der Zwaag, Tailoring the release of encapsulated corrosion inhibitors from damaged coatings: controlled release kinetics by overlapping diffusion fronts, Prog. Org. Coat. 75 (2012) 20–27, https://doi.org/10.1016/j.porgcoat.2012.03.002.
[129] P. Klomjit, R.G. Buchheit, Characterization of inhibitor storage and release from commercial primers, Prog. Org. Coat. 114 (2018) 68–77, https://doi.org/10.1016/j.porgcoat.2017.10.005.
[130] N. Madelat, B. Wouters, E. Jalilian, G. Van Assche, A. Hubin, H. Terryn, T. Hauffman, Differentiating between the diffusion of water and ions from aqueous electrolytes in organic coatings using an integrated spectro-electrochemical technique, Corros. Sci. 212 (2023) 110919, https://doi.org/10.1016/j.corsci.2022.110919.
[131] J. Mardel, S.J. Garcia, P.A. Corrigan, T. Markley, A.E. Hughes, T.H. Muster, D. Lau, T.G. Harvey, A.M. Glenn, P.A. White, S.G. Hardin, C. Luo, X. Zhou, G. E. Thompson, J.M.C. Mol, The characterisation and performance of Ce(dbp)3-inhibited epoxy coatings, Prog. Org. Coat. 70 (2011) 91–101, https://doi.org/10.1016/j.porgcoat.2010.10.009.
[132] G.M. Geise, D.R. Paul, B.D. Freeman, Fundamental water and salt transport properties of polymeric materials, Prog. Polym. Sci. 39 (2014) 1–42, https://doi.org/10.1016/j.progpolymsci.2013.07.001.
[133] S. Mondal, J.L. Hu, Z. Yong, Free volume and water vapor permeability of dense segmented polyurethane membrane, J. Membr. Sci. 280 (2006) 427–432, https://doi.org/10.1016/j.memsci.2006.01.047.
[134] M.F. Ferreira Marques, C. Lopes Gil, P.M. Gordo, Z.S. Kajcsos, A.P. de Lima, D. P. Queiroz, M.N. de Pinho, Free-volume studies in polyurethane membranes by positron annihilation spectroscopy, Radiat. Phys. Chem. 68 (2003) 573–576, https://doi.org/10.1016/S0969-806X(03)00234-2.
[135] S.Gh.R. Emad, S. Gad, Q. Ai, Y. Wan, S. Morsch, T.L. Burnett, Y. Liu, S.B. Lyon, J. Li, X. Zhou, Manipulating transport paths of inhibitor pigments in organic coating by addition of other pigments, Prog. Org. Coat. 172 (2022) 107072, https://doi.org/10.1016/j.porgcoat.2022.107072.
[136] S.Gh.R. Emad, X. Zhou, S. Morsch, S.B. Lyon, Y. Liu, D. Graham, S.R. Gibbon, How pigment volume concentration (PVC) and particle connectivity affect leaching of corrosion inhibitive species from coatings, Prog. Org. Coat. 134 (2019) 360–372, https://doi.org/10.1016/j.porgcoat.2019.05.008.